European Cells and Materials Vol. 43 2022 (pages 228-251) DOI: 10.22203/eCM.v043a16 ISSN 1473-2262

HISTOLOGY OF TENDON AND ENTHESIS – SUITABLE TECHNIQUES FOR SPECIFIC RESEARCH QUESTIONS

N. Angrisani[1,3,§,*], E. Willbold[1,3,§], A. Kampmann[2,3], A. Derksen[1] and J. Reifenrath[1,3]

[1] Hannover Medical School, Clinic for Orthopaedic Surgery, Hannover, Germany
[2] Hannover Medical School, Department of Oral and Maxillofacial Surgery, Hannover, Germany
[3] NIFE – Lower Saxony Centre for Biomedical Engineering, Implant Research and Development, Hannover, Germany
[§] These authors contributed equally to this work

Abstract

The musculoskeletal system consists of different components comprising a wide range of tissue types, with tendons being one part. Tendon degeneration or rupture have a high prevalence in all age groups, often with poor outcomes of surgical treatment such as chronic pain and high re-tear rates. Therefore, much effort has been directed to further develop diagnostic and therapeutic methods as well as reconstruction techniques, including using adequate placeholders or implants. Diagnostic approaches and advanced stages of preclinical studies will inevitably include histological examination of the pathologically affected tissue. The present study presents adequate tendon-related, histological techniques, including the embedding of soft- and hard-tissue samples in different media. Consideration is also given to samples containing residual implant materials or having been subjected to standard staining protocols and immunohistochemical procedures. The study further examines cells and tendon structure to detect degenerative, fibrotic or inflammatory conditions and possible foreign-body responses to implanted materials. Infraspinatus tendons from preclinical studies carried on rat and sheep samples, as well as human biceps tendon samples, have been used as example materials.

Keywords: Tendinopathies, hard tissue sectioning, histological evaluation, staining techniques.

***Address for correspondence**: Dr Nina Angrisani, Hannover Medical School, Clinic for Orthopaedic Surgery, Stadtfelddamm 34, 30625 Hannover, Germany.
Email: Angrisani.nina@mh-hannover.de

List of Abbreviations

AI	artificial intelligence
CD	cluster of differentiation
CSF1R	colony stimulating factor 1 receptor
EDTA	ethylenediaminetetraacetic acid
FBGC	foreign body giant cell
GAG	glycosaminoglycan
H&E	haematoxylin and eosin
IHC	immunohistochemistry
MEA	(2-methoxyethyl)-acetate
MNGC	mononucleated giant cell
MRC1	mannose receptor C-type 1
PCL	polycaprolactone
PMMA	polymethyl-methacrylate
UV	ultraviolet
TBS	tris-buffered saline

Introduction

The frequency of tendinopathies differs between different body regions. For example, in the general population, rotator cuff tendinopathy has been observed in 2-7 % of pathologies affecting the upper limb (Chard *et al.*, 1991; Miranda *et al.*, 2005), epicondylitis and medial epicondylitis have also been reported with a prevalence of up to 6.6 % (Tajika *et al.*, 2014). Tendinopathies are often triggered by repetitive movements (Kvist, 1994) and it is therefore not surprising that athletes seem to be the most frequently affected group and that differences in prevalence between athletes and workers are present (Hopkins *et al.*, 2016). Overall, tendinopathy has a considerable socio-economic impact (Vitale *et al.*, 2007). Tendon ruptures are complex injuries and

Table 1. Summary of samples used for depiction of staining results.

Sample origin	Predominant tissue	Sample size (max length × max width); in mm	Formalin fixation duration
Human	Tendon, connective tissue	8 × 5	2 d
Rat	Tendon, connective tissue, bone	10 × 5	2-3 d
Sheep	Tendon, connective tissue	20 × 10	4-5 d
Sheep	Tendon, connective tissue, bone	40-70 × 30	7-10 d

are often difficult to treat. Most commonly affected tendons are the Achilles tendons, the flexor tendons, the biceps tendon or the tendons of the rotator cuff (Florit *et al.*, 2019; Sobhani *et al.*, 2013; Thomopoulos *et al.*, 2015; Titan and Andarawis-Puri, 2016). The prevalence of rotator cuff tears positively correlates with age (Lawrence *et al.*, 2019). These tears often cause only moderate pain, which leads to a delayed medical consultation, at a time when changes of the tissues involved, such as tendon retraction, muscle atrophy or fatty infiltration, are already chronic. These chronic pathological changes often lead to poor surgical outcomes in the older age groups, with 11-94 % re-tears (Le *et al.*, 2014). Insufficient and unstructured repair tissue contributes to these failure rates.

The gap between tendon and bone after injury, which is often caused by the retraction of the tendon, needs to be bridged using an adequate placeholder that provides the required stability until the tissue has healed. Before entering clinical studies, development of such placeholders/implants will inevitably include preclinical *in vivo* studies to evaluate their impact on the organism, considering functional and biological performance. Here, histological examination plays a key role.

Tendons and their adjacent tissues show a wide range of tissue characteristics. Muscle tissue is soft and its properties differ depending on the current level of action. Tendons are more rigid than muscles and interconnect muscles with bones. The bone itself is the most rigid component, representing the whole organism supporting structure. These different tissue properties necessitate the use of different histological techniques for scientific investigations. Possibilities comprise of using frozen-section techniques, paraffin-wax section methods and plastic-embedded samples. The latter can be prepared using microtome cutting blades or applying the cutting and grinding method described by Donath and Breuner (1982).

When choosing the optimal histological technique, the enthesis constitutes a special challenge due to the presence of tissues with varying characteristics. It is possible, using subsequent optimised processing, to distinguish between the different bone, cartilage, tendon and muscle regions. However, examination of the transition zone is commonly the most important aspect.

This study systematically discusses histological techniques for processing enthesis and tendon tissue to optimally address a variety of research questions. The examination of cells as well as the structure of tendons were considered in order to assess degenerative, fibrotic or inflammatory conditions and possible foreign-body responses to implant materials. Human biceps tendons and infraspinatus tendons of preclinical studies (rat, sheep) are used as exemple materials.

Material/origin of sample tissue

The examples given in this study are based on tissue samples deriving from three different species. One part was taken during surgical shoulder replacement procedures carried out at the Clinic for Orthopaedic Surgery (Diakovere Annastift, Hannover Medical School, Hannover, Germany, ethical approval number 7281). All samples were transferred to the histological laboratory for further processing. The other samples derive from either rats or sheep. Both animal studies were part of the Research Unit "FOR 2180 - Graded Implants for Tendon-Bone Junctions", which aims to develop implants for the reattachment of ruptured tendons. This research project involved the establishment of a chronic rotator-cuff-tear model in rats (approval number 33.12-42502-04-15/2015) to evaluate the general tissue reaction to electrospun PCL mats without and with a different surface coating. Detailed description of this study and the surgical procedures used to implant electrospun PCL patches were published by Willbold *et al.* (2020).

For the evaluation of tendon implants in a sheep model (approval number 33.19-42502-04-17/2739), female black-headed mutton sheep underwent surgery to detach the infraspinatus muscle from the humeral head, which was either refixed immediately (acute defect model) or after 8 weeks (chronic defect model). Refixation was performed using non-resorbable suture anchors (FArthrex GmbH, Munich, Germany) using a double-row technique, a standard technique for human rotator-cuff-tear refixation surgery. 12 weeks after refixation, animals were euthanised and bone-tendon-muscle samples were excised and further processed for histology.

Embedding of samples

Tissue fixation

Prior to embedding, tissue fixation is required to preserve the cellular morphology. Despite its carcinogenicity, the most common fixative solution is buffered formalin. It is cheap as well as easy to store and handle. Beside formalin, there are numerous

other fixation solutions, including both single chemicals (such as ethanol) and multi-component fixation solutions (Bancroft *et al.*, 2018; Lawrence *et al.*, 2019; Shields and Heinbockel, 2019). Fixation by adequate storing in ethanol is as simple as with formalin but with lower biological hazards. However, especially for collagen, a clear influence of fixative type or fixation time was shown by Turunen *et al.* (2017). The study found that following ethanol fixation, collagen shrinkage and loss of alignment is much more pronounced than in formalin-fixed samples and also emphasised the need for careful choice of fixative (Turunen *et al.*, 2017).

Adequate sample fixation depends on sample size and characteristics such as density. Fast fixation limits autolytic processes leading to better histological visualisation (Shields and Heinbockel, 2019). The softer the tissue the easier it is for the fixative to penetrate. For bone tissue, sufficient time should be given for adequate penetration of the fixative.

Tissue specimen sizes, as well as fixation times, covered in this review differed according to tissue origin and content. Values are summarised in Table 1.

Cryopreservation

Cryosectioning is possible but uncommon for non-decalcified specimens. Standard cryosectioning procedures used for soft tissue often destroy hard tissues. Kawamoto (2003) established a method that also preserves hard tissue structures during cryosectioning. The method was subsequently further refined and new protocols published (Kawamoto and Kawamoto, 2020). To preserve tissue structure, thin plastic film templates are applied on the frozen sample prior to sectioning and the residual slice adheres to this film for further processing. This method has been used for bone characterisation by IHC, *e.g.* in offspring mice (Fecher-Trost *et al.*, 2019), and it would be possible to use it for tendon and enthesis as well. However, special expensive films are necessary, which have to be purchased from Kawamoto´s section lab (Web ref. 1). All staining methods described in this review are also possible on samples produced according to the Kawamoto technique. However, as this technique is rarely used, no exemple samples are produced and shown in the present review.

Paraffin-wax embedding

Paraffin-wax embedding is the most common embedding technique for nearly all tissue types and numerous staining protocols are available for such embedded sections. All paraffin-wax-embedded samples shown in the present study underwent a standard embedding protocol using Excelsior™ ES Tissue Processor (Thermo Fisher Scientific). Dehydration of the samples was achieved using an increasing alcohol series (propanol, 70 % for 1 h, 90 % for 1 h, 100 % 4 times for 1 h each). Alcohol and wax are immiscible, necessitating a further step. Specimens were rinsed in Xylol (3 times for 1 h each), a clearing agent which first replaces the alcohol and then is replaced by paraffin-wax. Embedding was completed by infiltration (at ~ 60 °C) of paraffin-wax, 3 times × 1 h each, changing medium each time. Next,

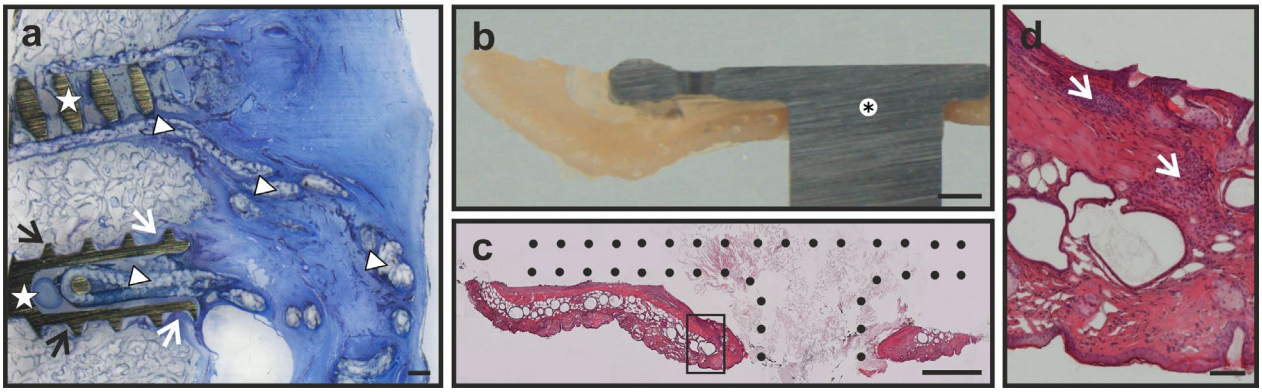

Fig. 1. Processing possibilities of tissue samples with metallic implants. (**a**-**c**) Scale bar: 1 mm. (**d**) Scale bar: 100 μm. (**a**) Metallic bone anchors (white stars) within a femoral head. The accompanying suture material (white triangles) outside (upper anchor) and inside (lower anchor) the screw is well recognisable. Note the close bone-to-implant contact in the distal part of the anchor (black arrows) in contrast to the cartilaginous tissue near the first thread (white arrows). Sheep, infraspinatus tendon refixed with suture anchors (double row technique); embedding in Technovit 7200, ground section, thickness of section 30 μm, toluidine blue. (**b**) Metallic implant (*) within the dermis. Mouse, embedding in Technovit 9100, not dissected and not stained tissue block before electrochemical removal of implant, reflecting-light microscope. (**c**) Same sample as in Fig. 1**b**, metallic implant dissolved by electrochemical dissolution. Former implant location (●) is devoid of material, dermal tissue can be evaluated in high resolution. Mouse, embedding in Technovit 9100, microtome section, thickness of section 4 μm, H&E. (**d**) Larger magnification of black square in Fig. 1**c**. Evaluation of cells in the tissue that was in direct contact with the implant prior to removal is possible. Inflammatory cells (predominantly neutrophil granulocytes) are visible (white arrows). Mouse, embedding in Technovit 9100, microtome section, thickness of section 4 μm, H&E.

the paraffin-wax blocks were mounted on a sample holder, which fitted into the microtome.

It is important to note that specimens that include bone tissue have to be decalcified before paraffin-wax embedding using chelation agents such as EDTA or acids. If small metallic implants or residual parts are present in the sample, a decision must be made whether the interconnecting zone is of interest or not. While some metal alloys, *e.g.* magnesium, would also dissolve during decalcification in EDTA, metals such as titanium or stainless steel have to be removed in advance. If the evaluation needs to include the direct bone-to-implant interface, the only possibility is embedding in plastic followed by the removal of metal compounds using electrochemical methods (Willbold *et al.*, 2013) or the application of a cutting-grinding technique.

Plastic embedding

Embedding in plastic is the preferred method when non-decalcified bone tissue or metal implants are part of the sample. Two principal types of plastic are available for the embedding of hard tissues and both are provided by Kulzer Technik (Wehrheim, Germany). A detailed description of embedding and staining of non-decalcified bone samples in Technovit 9100 is published by Willbold and Witte (2010).

Technovit 9100 comprises of several agents that have to be combined. Basic liquid (methyl methacrylate), powder (methyl methacrylate in dibenzoyl peroxide), hardener 1 and 2 (dicyclohexyl phthalate, di-benzoylperoxid and N,N,3,5-tetramethylaniline) and regulator (decane-1-thiol) polymerise in the cold (maximum of –2 °C, minimum of –20 °C) by excluding oxygen, therewith dissipating polymerisation heat (Rammelt *et al.*, 2007). While processing demands a more experienced technician, the resulting samples are suitable for all staining techniques. Also, the preparation of ground sections using a band saw and a micro grinder is possible. However, cold polymerisation of large sample sizes is challenging and the lower hardness compared to Technovit 7200 leads to a faster clogging of technical components during sawing and grinding.

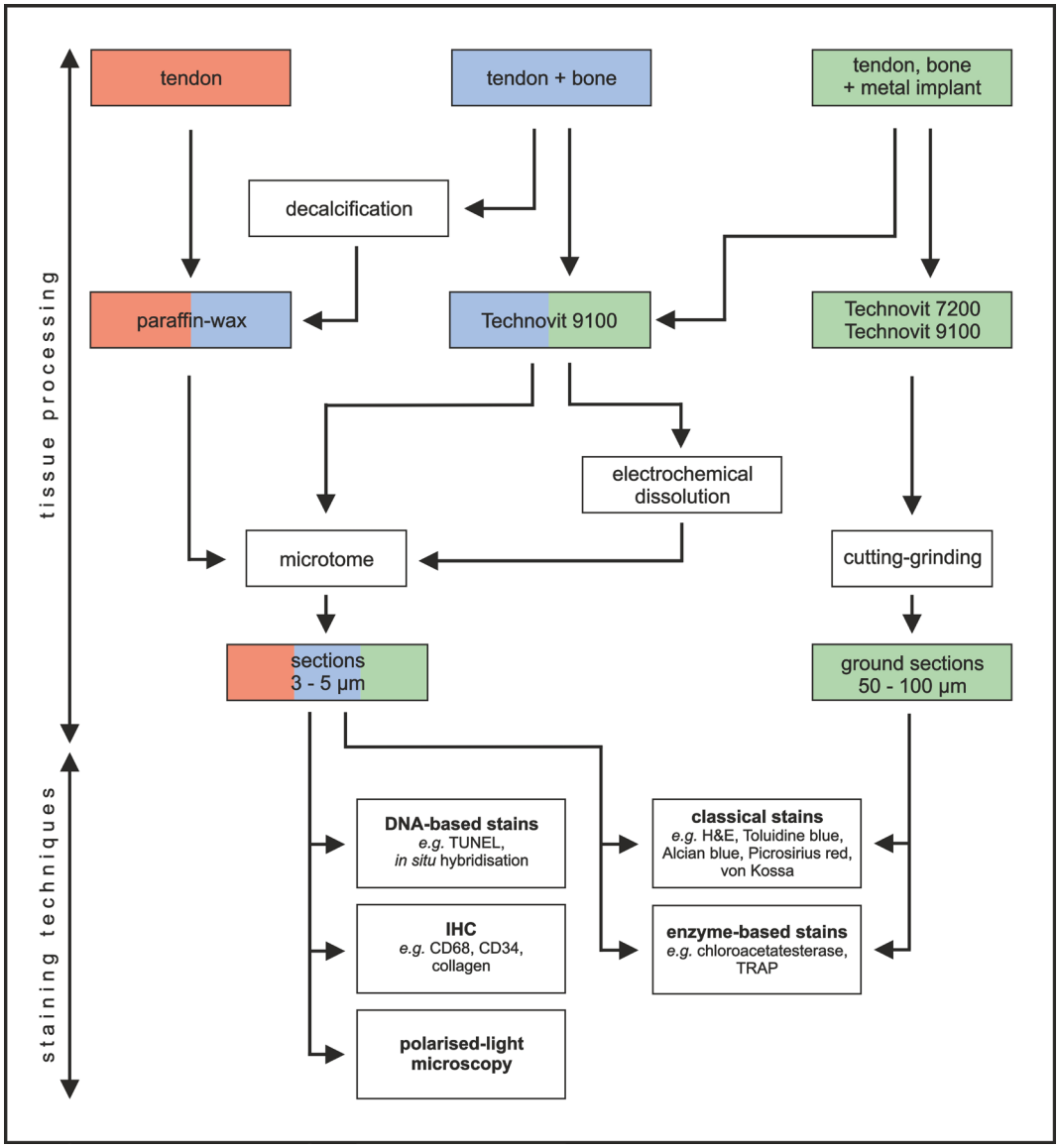

Fig. 2. Flowchart for tendon-tissue processing. The possible processing techniques and subsequent selection of staining for different tendon-related histological samples are depicted.

Table 2. List of advantages (Pros) and disadvantages (Cons) of the different embedding/sectioning techniques.

Technique		Pros	Cons
Microtome sectioning		Thin slices Nearly all staining techniques Cheap Easy	No metals Decalcification of hard tissues necessary
	Technovit 9100	Thin slices of hard tissue Nearly all staining techniques	Costs Time/numerous process steps
Cutting Grinding	Technovit 9100	Nearly all staining techniques, including IHC Preservation of tissue-implant interface	Costs/special equipment Thick slices/several cell layers per slice "Softer" plastic/soiling of equipment
	Technovit 7200 or other PMMAs	Preservation of tissue-implant interface Also big metallic implants cuttable	Costs/special equipment Thick slices/several cell layers per slice Only staining of surface/special protocols Experienced technician
Cryosectioning		Thin slices Nearly all staining techniques No influences of fixative on epitopes for IHC Easy/fast processing Cheap	No metals Hard tissue sections, possible only with specialised expensive foils Frozen storage necessary Lower quality compared to embedded samples

Beside Technovit 9100, another hard-plastic embedding medium – Technovit 7200 – is available with slightly different properties. The chemical component of Technovit 7200 is 2-hydroxyethyl methacrylate isobornyl methacrylate. It polymerises under UV light and is recommended especially for samples that include non-cuttable materials. Its advantages are the uncomplicated processing technique, the large possible sample size and the resulting properties of the embedded tissue block. The hardness of the sample is optimal for the preparation of ground sections prepared by a diamond band saw and micro grinder. However, due to the thickness of the final slice, only surface staining can be performed. While there are staining protocols for the most common dyes, IHC is also possible (Salles *et al.*, 2011) but more challenging and scarcely performed.

These differences are well depicted in Fig. 1. Fig. 1**a** shows a plastic-embedded sample, prepared by cutting and grinding, containing two titanium screws, which were part of the refixation of the muscle infraspinatus tendon at the humeral head in a sheep. Metal bone anchors with residuals of the adhering suture material are visible. For the refixation using the double-row technique, two different suture anchors were applied: Swive Lock®, self-punching, and Corkscrew®FT (both Arthrex, Munich, Germany). While the suture is well recognisable within the screw in the lower Corkscrew®FT anchor, it can be seen outside of the screw in the upper Swive Lock® anchor. Furthermore, the tight bone-to-implant contact can be seen at the lower threads of the lower screw, while there is a small area of cartilaginous tissue near the first thread (Fig. 1**a**). Fig. 1**b** also shows a metal implant implanted into the dermis. Here, the tissue-implant compound is embedded in Technovit 9100 and visualised using a reflecting-light microscope. After removal of the metal implant by electrochemical dissolution (Willbold *et al.*, 2013), the cutting of thin microtome sections is possible, enabling high-resolution microscopy for a detailed evaluation of cells (see enlargement, Fig. 1**d**) in direct vicinity to the former implant location, here depicted by points (Fig. 1**c**). Fig. 1**d** shows inflammatory cells in the contact area between implant and tissue. Alternatively, poly methyl methacrylate from other suppliers can be used for plastic embedding, *e.g.* polyscience Europe GmbH (Hirschberg an der Bergstraße, Germany) or Fluka Chemie GmbH, Buchs, Switzerland, as *e.g.* used by Plecko *et al.* (2012).

To help choosing the correct technique for embedding and staining of tendon-related tissue, a flowchart is provided that contains different processing possibilities for different tissue samples (Fig. 2). Table 2 displays the pros and cons for the different embedding possibilities according to the author´s experience.

Staining of samples

There are numerous staining protocols described in the literature. Different stains provide different information about the status of tissues and cells. Expertise needed and technical requirements increase

as well as chances of error with increasing specialty of the protocols. Therefore, careful consideration has to be given to choosing the favoured staining technique. Furthermore, the embedding and sectioning procedure determines the protocol that has to be followed. While there are staining protocols for nearly all common and also more specialised dyes for paraffin-wax-embedded samples, staining of plastic-embedded samples is typically more challenging.

Paraffin-wax- and Technovit 9100-embedded samples are usually cut by microtome to a thickness of around 4-5 µm. Before staining, in a first step, the embedding medium has to be removed and the tissue has to be rehydrated so that the dye can infiltrate the tissue. This is achieved in reverse order of the fixation and embedding process by using xylol followed by a decreasing-concentration alcohol series. Deplasticising Technovit-embedded samples would need a prolonged time span if only xylol is used. This time span can be shortened by performing an intermediate step with MEA before rehydrating.

Ground sections of Technovit-embedded tissue with a standard slice thickness of 50-100 µm have to be stained differently. Due to the thickness and, therefore, large amount of embedding medium, no removal is performed. The staining solution is applied directly onto the embedded sample, after a short etching procedure with formic acid, and it stains the superficial layer of the section. The greater thickness of the section decreases the available resolution because of light scattering within the sample and limits the examination of the sections to lower microscope magnifications. However, examinations at lower magnifications are suitable for cells in close proximity of implants or other soft-hard interfaces.

Staining methods depending upon the specific research question

In the evaluation of tendinopathies and related research, a successive approach is often followed: initially, the aim is a first assessment and overview diagnosis ("general overview"). Subsequently and based on the first diagnosis, a more thorough examination of tissue structure and cells will follow. Depending on the main focus, there are different possibilities for staining the samples. Fig. 3 gives an overview of the common staining techniques and their allocation to the three aforementioned sections.

A list of important staining techniques can be found at the end of the manuscript that provides basic information on their chemical composition and example references.

Overview: general screening of samples

The most common pathological changes in tendinopathy and tendon tears are loss of structure of the collagen fibres (Maffulli *et al.*, 2000; Scott *et al.*,

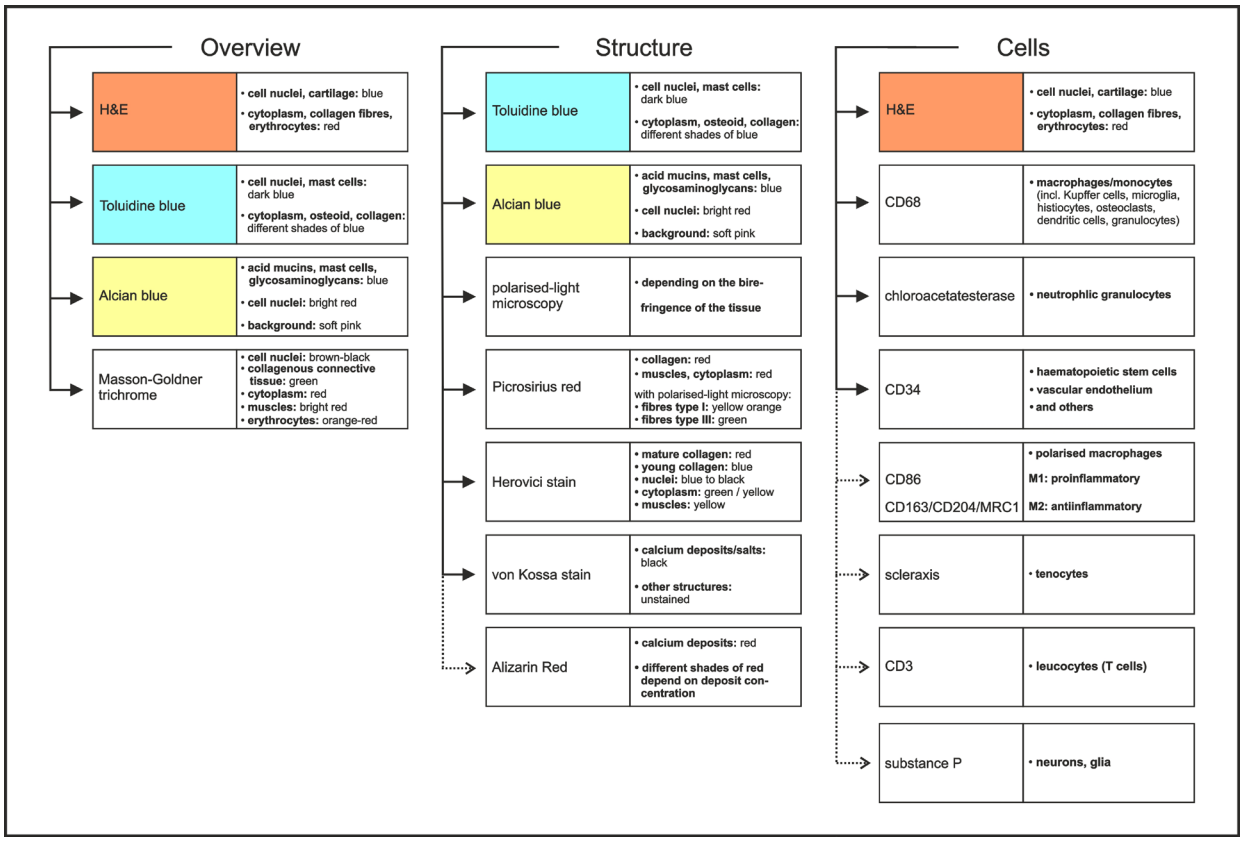

Fig. 3. Staining possibilities according to the underlying research question using the most common staining techniques. H&E (orange), toluidine blue (light blue) and alcian blue (yellow) are simple standard staining techniques that are common and can be applied for a first general evaluation (overview) as well as for deeper insight regarding structure and cells within the tendon tissue.

2015) as well as increased vascularity (Andersson *et al.*, 2007; Maffulli *et al.*, 2000; Matthews *et al.*, 2006), GAGs (Maffulli *et al.*, 2000) and more rounded tenocytes. For a basic evaluation of cellular reactions, the well-established standard dye-based staining techniques are most suitable. Routine pathological evaluation is predominantly done on H&E-stained samples. Following this methodology, most cells can be identified and a first impression of the tissue structure can be obtained. This method is also used in several research studies (Andersson *et al.*, 2007; Maffulli *et al.*, 2000; Matthews *et al.*, 2006). The same applies for toluidine blue. If bone tissue is part of the sample, toluidine blue offers additional information by staining different stages of mineralisation in different shades of blue, including calcification/chondral ossification of soft tissue parts. Notably, different immersion times in the staining solution can influence the tissue colouring. Therefore, a decision has to be made as to which part is of greater interest – bone/calcification or soft tissue. Fig. 4 shows a calcification/ossification location within the tendon of a muscle infraspinatus (inserting at the humeral head) in a sheep 12 weeks after refixation of the tendon. Fig. 4**a** shows a ground section that was stained with toluidine blue. The calcified part of the tendon is darkly stained and clearly visible in the centre of the image. It is surrounded by violet-stained regions where endochondral ossification of the tissue takes place. As typically observed in thicker ground sections, the cell types are harder to identify, especially in the outer region of the sample, which is deeply stained. In contrast to the ground section, Fig. 4**b**-**d** show microtome-cut sections of a corresponding calcification. Again, the region of endochondral ossification is obvious due to its lilac staining by toluidine blue (Fig. 4**b**) and also in H&E (Fig. 4**c**). Additionally, the thinner microtome-cut slices allow for a clear identification of the typically blebby and rounded appearance of the chondrocytes. Cells and structure of the adjacent tissue can be easily examined. The typically well-organised tendon structure is lost in the vicinity of the calcified area. Additional information is given using the von Kossa staining method (Fig. 4**d**), a very common method for detecting and depicting calcifications (Carvalho *et al.*, 2020; Schneider, 2021; Wu *et al.*, 2020; Zegyer *et al.*, 2020). Calcium, which is present as carbonates and phosphates, is replaced by silver ions, which are subsequently reduced to metallic silver in the presence of light. Therewith, calcifications are displayed in black. The most important advantage of this technique is that even small zones of calcifications are reliably detected. Due to the clear difference between black colouring and the other tissue, automated analysis using computer programs is possible and easy to perform. On the other hand, the black colouring also constitutes the biggest disadvantage because in the area of the von Kossa-stained tissue an examination of cells is no longer possible. This fact is well illustrated in Fig. 4**d** where the whole extent of mineralisation is captured by von Kossa staining. To gain further information about the cells in the periphery of the calcification, which is not stained by von Kossa, different dyes for counterstaining are available (Limraksasin *et al.*, 2020).

Another stain used for the depiction of calcifications is alizarin red (Dai *et al.*, 2020). Compared to von Kossa, alizarin red staining still enables the

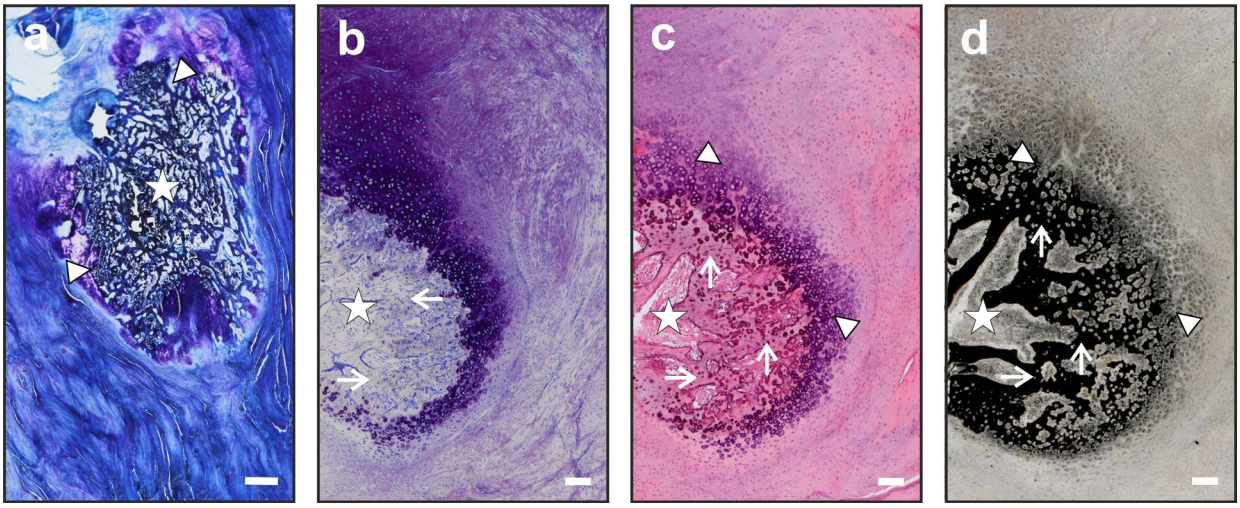

Fig.4. Area of calcification in the tendon of muscle infraspinatus (sheep) after refixation. (**a**-**d**) Scale bar: 1 mm. (**a**) Calcified part of the tendon (white star) is visible in the centre, surrounded by lilac-stained regions (white triangles) of endochondral ossification. Sheep, infraspinatus tendon refixed with suture anchors (double row technique), embedding in Technovit 7200, ground section, thickness 30 µm, toluidine blue. (**b**-**d**) Endochondral ossification is well recognisable (white triangles) in the outer region of the central area of calcified tissue (white stars). The thinner microtome sections enable recognition of osseous trabeculae in the centre (white arrows). (**d**) However, cells are not visible in the deeply-black-stained areas of calcified tissue in the von Kossa-stained sample. (**b**-**d**) Sheep, infraspinatus tendon refixed with suture anchors (double row technique), embedding in Technovit 9100, microtome section, thickness 4 µm. (**b**) Toluidine blue, (**c**) H&E, (**d**) von Kossa.

assessment of the structure within the calcified area due to its greater relative transparency. However, it is not a commonly used dye in the histological evaluation of tendon tissue but rather in cell culture tests (Yin *et al.*, 2019) or skeletal staining (Rigueur and Lyons, 2014).

Masson-Goldner trichrome and picrosirius red are further basic or standard-dye-based staining methods. These techniques can be complimentary to a first step tissue assessment using H&E and/or toluidine blue. Masson-Goldner trichrome clearly distinguishes between all different kinds of tissue (mineralised bone, newly formed bone, cartilage, muscle/connective tissue) and rapidly reveals the tissue structure. Its value for orthopaedic samples that include tendon tissue is due to its good affinity for collagen fibres (Courtoy *et al.*, 2020). However, if fibrillary collagen is involved, picrosirius red is advantageous due to its higher binding affinity (Lattouf *et al.*, 2014). The clear contrasting of collagens from the adjacent tissue enables the effective and reliable examination of fibrosis (Huang *et al.*, 2013).

Although alcian blue can be considered as a basic staining regarding cell visibility, it gives additional information on the amount of both sulphated GAGs and non-sulphated hyaluronan, represented by a more blue/less red staining in samples with a large content of GAGs (Maffulli *et al.*, 2000). Fig. 5 shows the insertion area of tendons at the humeral head 12 weeks after reattachment in a sheep model and it displays the same region of enthesis stained with toluidine blue, Masson-Goldner trichrome, alcian blue or picrosirius red. The additional information provided by the respective dye is clearly visible. While toluidine blue (Fig. 5**a**) already gives a good overview of the structure and cells, Masson-Goldner trichrome (Fig. 5**b**) visualises small vessels and the transition zone from unorganised collagen or fibrous tissue to the bone. In both alcian blue and picrosirius red stainings, a first assessment can be carried out at low magnification and taking advantage of the strong contrast between the predominating colours (Fig. 5**c**,**d**).

Structure

Tendons exhibit a special and unique physiological structure, which is described in detail by others (Thorpe *et al.*, 2013). Their structure of almost exclusively parallel type I collagen fibrils is one of the simplest in connective tissues (Svensson *et al.*, 2017) and provides optimal transfer of forces from muscles to bones. One of the main reasons underlying surgical failure rates following refixation of ruptured tendons is unstructured and insufficient repair tissue. This emphasises the importance of evaluating tendon structure. A straightforward technique for doing so is polarised-light microscopy as it only requires a specialised microscope. The highly ordered

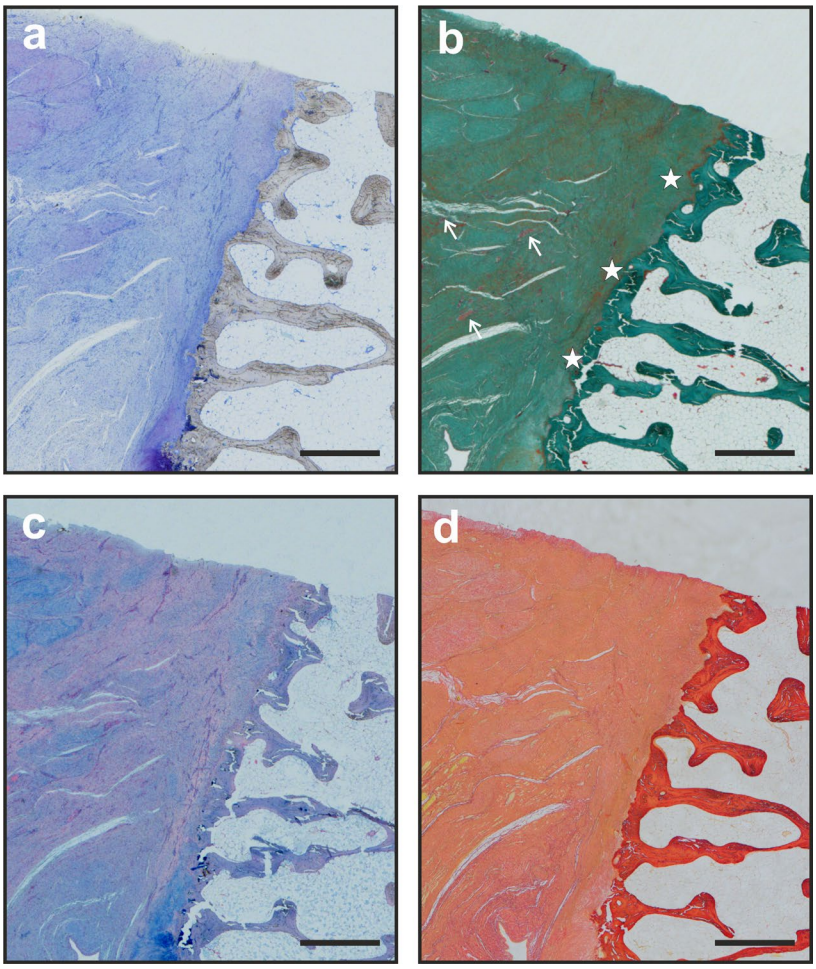

Fig. 5. Comparison of standard dye-based staining techniques, insertion of muscle infraspinatus at humeral head of sheep. (**a**-**d**) Scale bar: 1 mm. (**a**) Overview of structure and cells. (**b**) Small vessels (white arrows) and fibrocartilaginous transition zone (white stars) recognisable. (**c**) Areas containing hyaluronic acid and chondroitin sulphate in blue. (**d**) Depiction of muscle tissue in yellow, visible in the left part of Fig. 5**d**, with single strands inserting into the unorganised healing tissue near the bone, which is stained deep red. (**a**-**d**) Sheep, infraspinatus tendon refixed with suture anchors (double row technique), embedding in Technovit 9100, microtome sections, thickness 4 μm. (**a**) Toluidine blue, (**b**) Masson-Goldner trichrome, (**c**) alcian blue, (**d**) picrosirius red.

molecular structure of collagen fibres exhibits birefringence, which can be detected very effectively by polarised-light microscopy. A combination with staining techniques, such as picrosirius red, can further accentuate different structures (Junqueira *et al.*, 1979).

Fig. 6 shows the structure of the transition zone from muscle to tendon of the infraspinatus muscle. The sample derives from a sheep that underwent refixation of the detached tendon and a subsequent post-surgical period of 8 weeks. In Fig. 6**a**, picrosirius red staining allows a clear distinction between muscle (yellow) and tendon tissue (red). The combination of this stain with the simultaneous observation by polarised-light microscopy enables a very clear detection of the structure.

A further simple and useful technique for the visualisation of collagen is the Herovici stain (Michel *et al.*, 2020; Pei *et al.*, 2015; Teuscher *et al.*, 2019). In contrast to picrosirius red or other non-IHC staining techniques, mature (red-stained) and immature (blue-stained) collagen can be distinguished by Herovici staining (Pei *et al.*, 2015). Therefore, it allows the maturation process of new tendon tissue to be followed (Michel *et al.*, 2020). Fig. 7 gives two examples of Herovici-stained tendon samples. Fig. 7**a** shows the typical structure of a mature tendon next to some loose connective tissue containing many fat cells, while Fig. 7**b** depicts a part of a pathological human biceps tendon. In this unorganised tissue, both immature and mature collagen fibrils are present, as shown by the red- and blue-stained areas, respectively.

For all tendons, normal or abnormal, the most critical part of the tendon is its insertion into the bone, called the enthesis (Font Tellado *et al.*, 2015; Moffat *et al.*, 2008; Shaw and Benjamin, 2007). Because of the distinct tissue properties, stresses at the enthesis are highly concentrated (Font Tellado *et al.*, 2015) and injuries are very common and difficult to treat (Moffat *et al.*, 2008; Shaw and Benjamin, 2007). Entheses of tendons can be classified as either fibrous or fibrocartilaginous entheses (Claudepierre and Voisin, 2005). While tendons that connect to the metaphysis or diaphysis generally do so through fibrous entheses and play a minor role in tendinopathy, most tendons that connect to the epiphysis are fibrocartilaginous entheses (Claudepierre and Voisin, 2005). The sequence of cells from tendon to bone is recurring, as described by *e.g.* Marinovich *et al.* (2016). The zone of clearly aligned collagen fibres represents the dense connective tissue of the tendon. It is followed by the zones of uncalcified and calcified fibrocartilage, which are sharply separated from each other. This separation line is called the tidemark (Benjamin and McGonagle, 2001; Marinovich *et al.*, 2016). A single enthesis can exhibit both fibrous and fibrocartilaginous sites (Benjamin and McGonagle, 2001). As for tendon tissue, entheses are also mostly avascular and, thus, refixation of tendon or ligament is difficult due to the associated poor potential for regeneration (Bridgewood *et al.*, 2021; Campbell *et al.*, 2019; Connizzo *et al.*, 2013).

Fig. 8 shows the physiological and pathological appearance of the entheses of the muscle infraspinatus at the humeral head of rats. On the right side (Fig. 8**a**,**b**) a physiological enthesis is seen, with the fibrocartilaginous transition zone and the tidemark clearly visible. The conjunction of the fibrils to the bone tissue is already well recognisable in the upper, H&E-stained sample. The polarised-light microscopy image below only reveals how deeply they extend

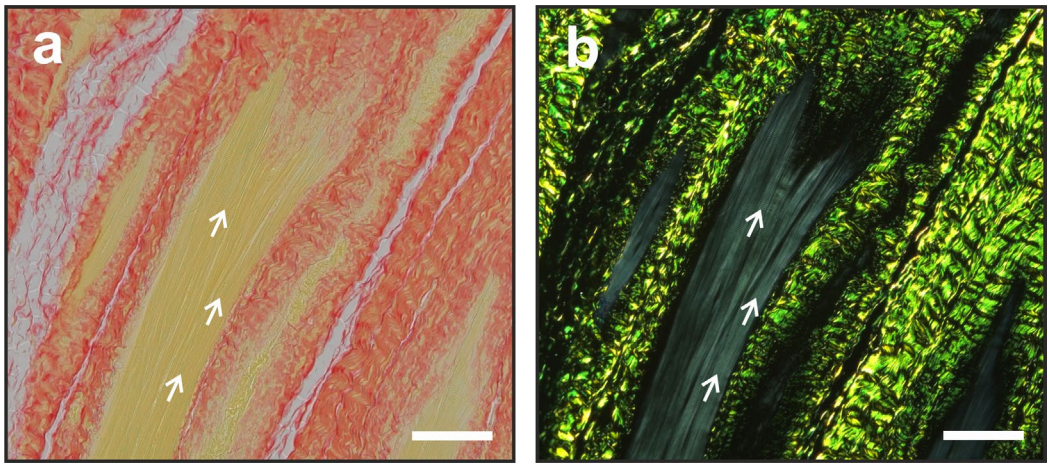

Fig. 6. Comparison of solely picrosirius-red-stained sample and supplementary imaging by polarised-light microscopy. Tendon-muscle transition zone, sheep. (**a**,**b**) Scale bar: 100 μm. (**a**) The tight contact between muscle tissue (yellow) and collagen fibres is visible but no transverse bands (white arrows) pointing out where bands should be. (**b**) Slide from 6**a** viewed by polarised-light microscopy. The formerly yellow areas of muscle tissue is dark but shows the typical transverse bands (white arrows). The collagen fibres of tendons of picrosirius-red-stained samples is depicted green-yellowish and accentuates the alignment of the fibres. (**a**,**b**) Sheep, infraspinatus tendon refixed with suture anchors (double row technique), embedding in Technovit 9100, microtome sections, thickness 4 μm. (**a**) Picrosirius red. (**b**) Picrosirius red and polarised-light microscopy.

into the bony tissue. On the right side (Fig. 8 **c**,**d**), a sample of the same tendon is shown but 8 weeks after refixation. The main difference can already be seen in the conventionally stained sample: there is no typical transition zone from tendon to bone. The uncalcified fibrocartilage is almost missing and there are no fibrillary extensions that bridge the tidemark to conjoin to bone tissue. Polarised-light microscopy confirms these findings, as no birefringent structures could be seen in calcified fibrocartilage or bony tissue. Although the cellular details cannot be seen with the same high resolution, ground sections offer a valuable and often impressive visualisation of the enthesis. They are particularly useful for samples derived from large animals such as sheep, which are usually too large to show an adequate area on one slide. Therefore, the best solution is often to divide the sample into two parts. One part serves for an evaluation of the whole enthesis while the other part is processed and cut by microtome to allow an assessment of cells. Fig. 9 shows ground sections of sheep tendons. Fig. 9**a**,**b** exhibits the common patterning of uncalcified and calcified fibrocartilage and tidemark.

Cells

Tendon healing is separated into three steps: inflammation, proliferation and remodelling (Chisari *et al.*, 2020; Jomaa *et al.*, 2020). While the inflammation phase should not last longer than weeks, its regulated presence is of great importance for the healing process and the structure of the tendon (Jomaa *et al.*, 2020). Tendinopathy could be understood as a failed healing process (Fu *et al.*, 2010) often associated with a prolonged/chronic phase of inflammation. Macrophages belong to the first line of defence in innate immunity. They play important roles in both healing and inflammation and, in case of the latter, are essential contributors to its resolution (Mantovani *et al.*, 2013). To resolve inflammatory processes, one of the main functions of macrophages is phagocytosis of debris and apoptotic neutrophils (Bystrom *et al.*, 2008). They also play a major role in eliminating foreign material such as degradable implants or dissolving suture materials. Resident macrophages have an irregular cell boundary, an oval, eccentrically located nucleus and dense chromatin (Mescher, 2017). Usually, they have many lysosomes. Due to these features, an experienced investigator could identify macrophages in physiological tissues using standard staining techniques such as Masson-Goldner trichrome (Benjamin and McGonagle, 2007). However, in a pathological situation, hypercellularity of different cell types is often present and differentiation is more difficult. Furthermore, within loose connective tissue, they could resemble fibroblasts and could be misidentified as such.

FBGCs arise from the fusion of macrophages and are almost always found when large foreign bodies are present. Due to their typical structure, FBGCs are easily recognisable even following toluidine blue or H&E staining. The multinucleated cells show a large inner area of few cellular structures and, therefore, low staining intensity while the nuclei are gathered at the outer edges of the cell. Fig. 10**a** shows a massive invasion of FBGCs following the implantation of PCL fibre mats in rats (toluidine blue). While these multinucleated cells are easily recognisable, especially in pathological tissues, the presence of macrophages or MNGCs (Al-Maawi *et al.*, 2018) is more difficult to assess. Often there are multiple cell types and disorganised tissue in the area of interest and a quantitative analysis of the appearance of macrophages based on the use of standard dye-based staining protocols is difficult. In this context, IHC

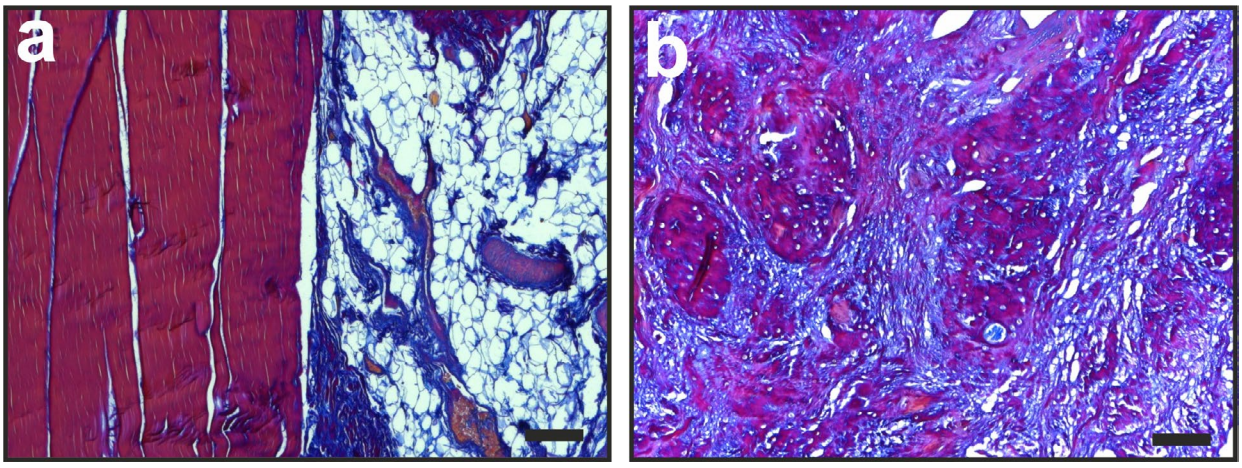

Fig. 7. Distinguishing mature and immature collagen fibres using Herovici stain. (**a**,**b**) Scale bar: 100 μm. (**a**) Typical structure of a mature tendon (red/pink-stained area on the left side) next to some loose connective tissue containing many fat cells (right side). (**b**) Part of a pathological human biceps tendon with unorganised tissue. Immature (blue stained) and mature (red stained) collagen fibrils are present and mingled closely with each other. (**a**,**b**) Human tendon biopsies, part of biceps tendon of a patient with aseptic bursitis, embedding in Technovit 9100, microtome section, thickness 4 μm.

represents the best option. The IHC working principle is to choose a specific primary antibody that binds to the tissue antigen of interest. The visualisation of the primary antibody can be achieved in different ways, either directly, by labelling of the primary antibody with a fluorescent dye or an enzyme, or indirectly by using a secondary antibody that binds specifically to the primary antibody. The secondary antibody is labelled and – due to the use of two antibodies – an additional step is necessary.

All standard immunohistochemical protocols are designed for paraffin-wax-embedded or frozen samples, whereas protocols for plastic-embedded samples often have to be established by adapting paraffin-wax protocols. As mentioned before, a PMMA that polymerises in the cold (*e.g.* Technovit 9100) should be used to avoid protein denaturation due to emission of polymerisation heat.

Tissue processing must be performed with great care to achieve satisfactory results (Ward and Rehg, 2014). Usually, the target tissue antigens are proteins that are sensitive to cross-linking and denaturation. Only frozen sections preserve those antigens unaltered. For paraffin-wax and plastic sections, the fixative solution and the embedding parameters, such as temperature, are important. Fixation is performed by the crosslinking of proteins, including the antigens of interest. Therefore, antigen retrieval is the first mandatory step in nearly all IHC protocols except for cryo-sections. It depends on different parameters, such as antigen of interest, type of tissue, primary antibody used and type and duration

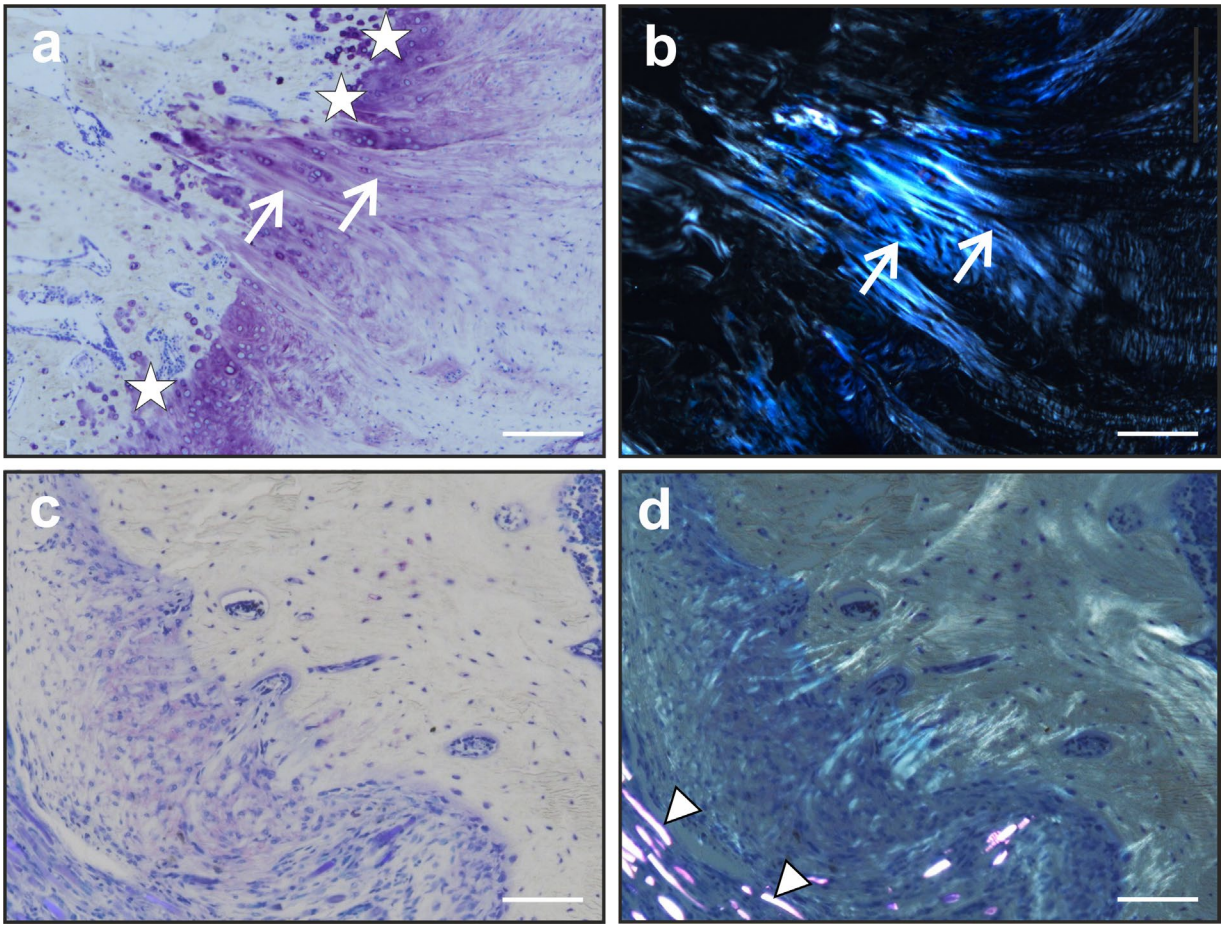

Fig. 8. Enthesis of muscle infraspinatus to humeral head of a (a,c) native and (b,d) refixed tendon. (**a**-**d**) Scale bar: 100 μm. (**a**) Physiological enthesis is clearly visible with the fibrocartilaginous transition zone and the tide mark (white stars). The conjunction of the fibrils to the bone tissue is already well recognisable (white arrows). Microtome section, H&E. (**b**) The polarised-light microscopy image of Fig. 8**a** emphasises the deep insertion of the fibrils into the bony tissue (white arrows). (**a**,**b**) Sheep, infraspinatus tendon refixed with suture anchors (double row technique), embedding in Technovit 9100, microtome sections, thickness 4 μm. (**a**) H&E, (**b**) H&E and polarised-light microscopy. (**c**) Pathophysiological situation of the refixed infraspinatus tendon of a rat 8 weeks after surgery. No typical transition zone from tendon to bone is recognisable, especially with missing fibrocartilaginous zone and no collagen fibrils that extent into the bone. (**d**) Polarised-light microscopy of Fig. 8**c** enables visualisation of collagen fibrils and their junction to the bone. In comparison to the physiological tissue their orientation is less directional. In the lower part of **d** highly polarising residues of the suture material are visible (white triangles). (**c**,**d**) Rat, infraspinatus tendon refixed with suture and a polycaprolactone-fibre scaffold, embedding in Technovit 9100, microtome sections, thickness 4 μm. (**c**) Toluidine blue. (**d**) Toluidine blue and polarised-light microscopy.

of fixation. There are two main different antigen-retrieval methods available: the proteolytic induced epitope retrieval using enzymes such as proteinase K, trypsin or pepsin, and the heat-induced epitope retrieval using different buffers and pH values (or a combination of both). The most commonly used buffers are citrate buffer (pH 6) or EDTA-containing buffer (pH 8) but there are also different commercially available retrieval solutions. Each protocol must be optimised for each tissue, fixation method and antigen to be studied and, generally, the heat-induced epitope retrieval method has higher success rates than the proteolytic induced epitope retrieval method, especially in the case of soft tissues. However, especially for samples with a large proportion of hard tissue, such as orthopaedic samples, the heat-induced epitope retrieval method has to be performed with great care: boiling destroys the tertiary structure of collagen, which has to be considered during the choice of antibody. Furthermore, the sections are severely affected by the cooking process.

The choice of the primary antibody depends on the species of origin. For example, primary antibody deriving from mice cannot be used for murine samples due to unspecific binding to numerous proteins present in the sample. There are protocols for using antibodies on species out of which they derived (*e.g.* Mouse on Mouse Polymer IHC KIT, abcam, Cambridge, UK, product number ab269452) but it is complicated and elimination of the background staining is very difficult. Blocking of non-specific binding to endogenous proteins is a step which is necessary to avoid unwanted, non-specific staining of the tissue background. Usually, serum of the origin species of the secondary antibody is used for this.

All staining procedures should be accompanied by positive and negative control samples. Positive control samples are tissue probes, which are known to contain the antigen of interest (*e.g.* spleen samples for macrophages), while negative control samples are tissue probes which definitively do not contain the antigen of interest. Negative antibody controls are necessary to exclude non-specific signals caused by non-specific antibody interactions with cellular components. Often, normal (non-immune) serum that is free of antibodies to the antigen of interest, or better, isotype antibodies that lack specificity to the target but match the class and type of the specific primary antibody are used. In cases where these reagents are not available, negative controls can also be prepared by leaving out the primary antibody while all other steps are performed. Principles and pitfalls of IHC are well described in Web ref. 2. For the identification of macrophages, common antibodies are anti-CD68, anti-CSF1R, anti-MRC1 and with slightly different specificity anti-CD86 and – especially for mice – anti-F4/80 (Barros *et al.*, 2013; Gordon *et al.*, 2011; Mauro *et al.*, 2016). Fig. 10**b** shows a similar area of the same sample as Fig. 10**a** but stained with anti-CD68. FBGCs are even more recognisable than in Fig. 10**a** and, additionally, singular macrophages can be identified.

As for other stains with distinct colour-contrasting, computer-assisted analysis of the stained areas is also possible. Programs such as Image J (public domain), Visiopharm software (Hørsholm, Denmark), Developer XD software (Definiens, Germany) or similar are capable of recognising different colours and can calculate parameters such as intensity ratios as quantitative values (Brown *et al.*, 2019; Podszun *et al.*, 2020).

Another cell type that plays an important role in innate and adaptive immunity are mast cells (Krystel-Whittemore *et al.*, 2016). After binding to a pathogen, they release inflammatory mediators for its elimination *e.g.* histamine, heparin, cytokines

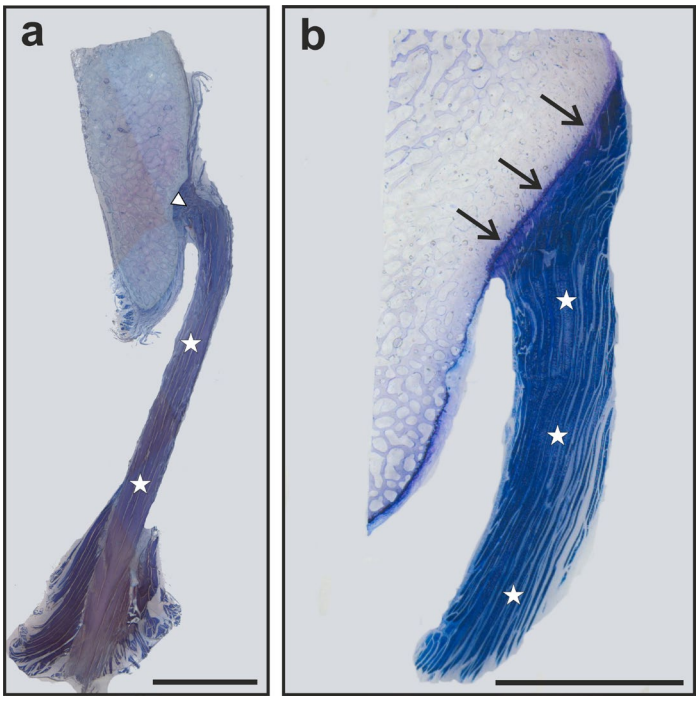

Fig. 9. Depiction of the physiological insertion of infraspinatus muscle at the humeral head in sheep. (**a**,**b**) Longitudinal section of the tendon and adhering bone with clearly structured collagen tissue (white stars), scale bar 10 mm. (**a**) Well recognisable footprint of the tendon at the femoral head (white triangle). (**b**) The fibrocartilaginous transition zone and the tidemark are clearly visible (black arrows) as well as the aligned collagen tissue of the tendon (white stars). (**a**,**b**) Sheep, native/healthy infraspinatus tendon, embedding in Technovit 7200, ground section, thickness 30 µm, toluidine blue.

and others (da Silva *et al.*, 2014). As discussed by Alim *et al.* (2020), mast cells contribute to neurogenic inflammation and the inflammatory reaction during tendon healing. Due to the metachromatic properties of the granules in which the mediators are stored in the cytoplasm of the cells, they are well recognisable already using toluidine blue staining. Up to 200 granules will appear violet-red, which is very eye-catching (Fig. 10**c**).

Beside mast cells and macrophages/FBGCs, neutrophil granulocytes are often present during inflammatory processes. In the presence of a foreign body such as an implanted biomaterial, they release proteolytic enzymes or reactive oxygen species and also try to participate in the phagocytotic processes (Labow *et al.*, 2001; Mariani *et al.*, 2019). Similar to the detection of macrophages, neutrophil granulocytes as part of a reactive, cell-rich tissue are not easy to detect and quantitative assessment requires further enhancement. In this context, chloroacetate esterase staining, as an enzyme-based staining technique, provides enhanced detection of neutrophils. Fig. 10**d** shows numerous neutrophil granulocytes in a sample of a human biceps tendon that was excised during surgical treatment of an aseptic bursitis.

Vascularity is a further highly important aspect during the examination of tendon tissue samples. Oxygen and nutrient supply are essential for the healing process as well as for the integration of biomaterials (Gniesmer *et al.*, 2019; Laschke *et al.*, 2006). In non-pathological tendons, especially in the distal part of the infraspinatus and supraspinatus tendons of the rotator cuff, vessels are scarce (Brooks *et al.*, 1992) and are present predominantly in the paratenon (Scott *et al.*, 2015). An increased number of vessels is a prominent feature in histopathology of tendinopathy often associated with neoinnervation (Xu *et al.*, 2011). As already mentioned, an increase in vascularity is also associated with healing processes, as demonstrated for example by Matthews *et al.*

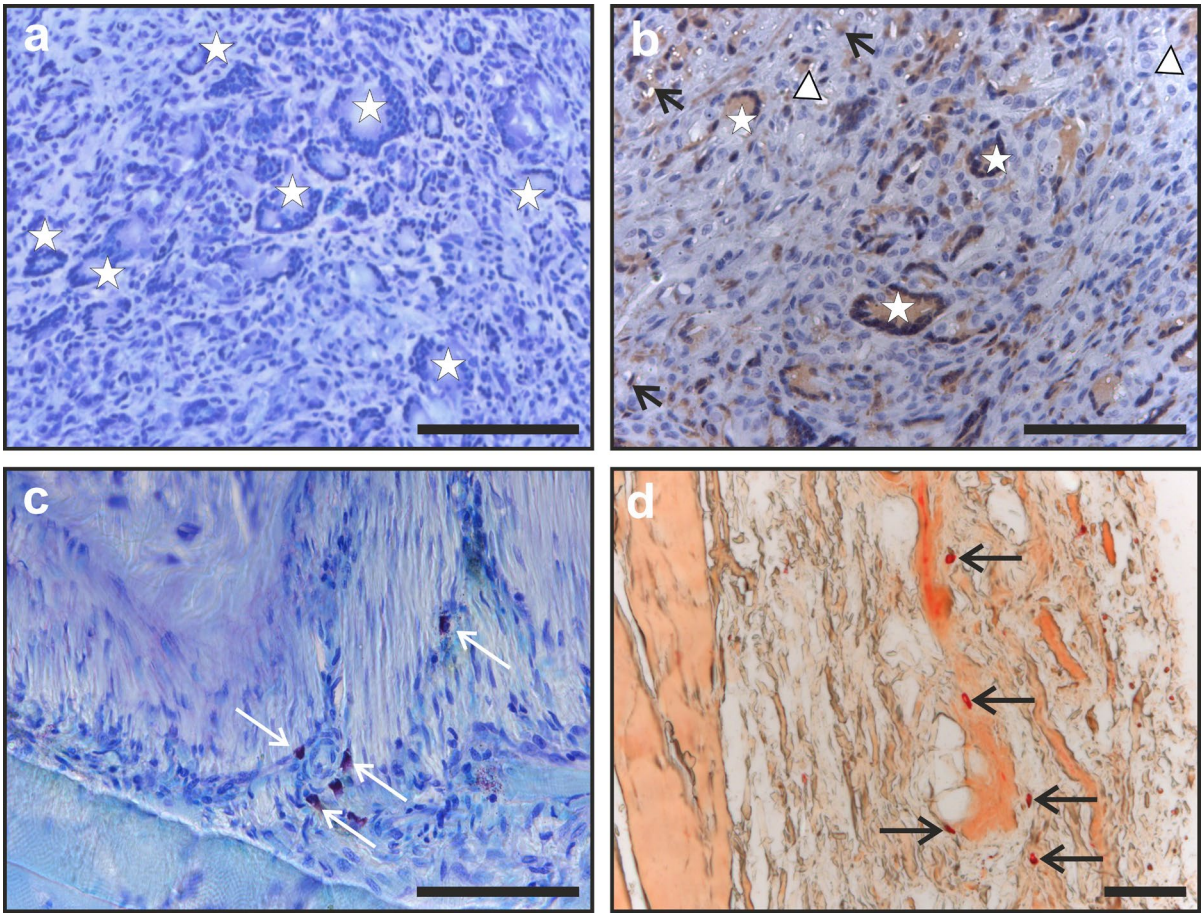

Fig. 10. Depiction of different cellular reaction within tendon tissue. (**a-d**) Scale bar: 100 μm. (**a**) FBGCs within reparation tissue of a refixed tendon in a rat model. (**b**) Similar area as 9**a**, labelled using IHC. The macrophage-directed antibody is secondarily labelled using diaminobenzidine, which enables clear identification of not only FBGCs (white stars) but also macrophages (black arrows) and mononucleated giant cells (white triangles). (**c**) Depiction of mast cells (white arrows) using the metachromatic properties of toluidine blue staining. (**d**) Occurrence of numerous neutrophil granulocytes (black arrows) as sign of an ongoing inflammatory process within a sample of human aseptic bursitis. (**a-c**) Rat, infraspinatus tendon refixed with suture and a polycaprolactone-fibre scaffold, embedding in Technovit 9100, microtome sections, thickness 4 μm. (**a**,**c**) Toluidine blue, (**b**) anti-CD68-diaminobenzidine and toluidine blue. (**d**) Human tendon biopsy, part of biceps tendon of a patient with aseptic bursitis, embedding in Technovit 9100, microtome section, thickness 4 μm, chloroacetate esterase staining.

(2006), who showed a decreasing number of vessels with increasing tendon tear size, indicating more reparative processes in smaller tendon tears.

Blood vessels, often with erythrocytes in the vessel lumen, can be identified using standard staining techniques such as H&E or toluidine blue. To assess their distribution within the tissue or quantitate them is time-consuming and requires an experienced, concentrating observer. Furthermore, obliquely cut vessels may complicate the evaluation. Therefore, IHC is often performed to detect vessels. A very common antibody for their detection in tendon tissue is anti-CD34 (Handa *et al.*, 2003; Matthews *et al.*, 2006; Zabrzynski *et al.*, 2018). Fig. 11 shows a human tendon sample taken from the long part of the musculus biceps brachii. In Fig. 11**a**, the tissue is stained with H&E, showing a pathologically highly vascularised tissue with further cell infiltrations. Fig. 11**b** shows accentuated vessels by fluorescence-coupled immunostaining of the endothelial cells using anti-CD34 antibody, which makes it easy to count and measure the diameter of the blood vessels. As anti-CD34 also binds to haematopoietic progenitor cells and leukocytes, these cells could also be counted.

Other staining techniques used for tendon tissue evaluation

The staining techniques discussed so far do not represent a complete description of all possibilities regarding tendon tissue evaluation. However, the present review describes the most commonly used staining techniques that enable a precise and already broad histological evaluation of tendon tissue samples. Moreover, it considers both structural and cellular assessment.

For further evaluation of special cells or other structural components as well as inflammation or differentiation state, there are numerous other stains and antibodies which could provide a deeper insight, *e.g.* staining of differently polarised macrophages (Dakin *et al.*, 2012), lymphocytes/tenocytes/histiocytes (Terada, 2012), collagen content, especially collagen type I or type III (Galatz *et al.*, 2006, Ge *et al.*, 2020), nerves for example by detection of neuropeptides such as substance P (Ackermann *et al.*, 2003), special glycoproteins such as tenascin or scleraxis as markers of proliferation/regeneration (Nakanishi *et al.*, 2019) or inflammatory markers such as interleukin-1 or interleukin-6 (Shi *et al.*, 2019).

Scoring systems for semiquantitative evaluation of tendinopathies

There is a wide range of scoring systems that are used to evaluate tissue characteristics in tendinopathies and different reviews already exist on this topic. Therefore, the present review only provides a brief overview by summarising some valuable references regarding scoring systems.

Different scores are used by different groups and to answer different research questions. Therefore, comparison of different studies is often difficult. For example, Roßbach *et al.* (2020) defined five variables such as fibre structure, fibre arrangement, rounding of nuclei, regional variations in cellularity and increased vascularity. They applied a 4-point scoring system that used values from 0 (normal appearance) up to 3 (markedly abnormal appearance). Then, the values for the different variables were summed to a total value ranging from 0 to 15 (Roßbach *et al.*, 2020). This scoring system was adapted from Longo *et al.* (2008).

Review articles on scoring systems could help when deciding on which score should or could be used. There are two broader review articles published by Loppini *et al.* (2015) and Titan and Andarawis (2016). The systematic review by Loppini *et al.* (2015) evaluated histopathological scores for tissue-engineered, repaired and degenerated tendons. They recommend the Movin score and its modifications to assess degenerative changes, as for example done by Tsang *et al.* (2019). On the other hand, they recommended the Soslowsky, Watkins, Novel and Burssens scores to evaluate tendon repair processes. In their opinion, the Matthys score assesses the histological changes in enthesopathies and the modified Watkins score has been well applied to assess enthesis repair (Loppini *et al.*, 2015).

In their review on scoring systems for tendinopathy, Titan and Andarawis (2016) found that collagen organisation was the only criterion assessed by every scoring system they implemented in their review. Vascularity and cellularity were the next most common markers evaluated, with 5 of the 7 scales taking these morphological changes into account. Cell morphology, continuity and fibrocartilage were used in 3 of the 7 scales.

This short paragraph already shows how many possibilities exist and are applied to assess histopathological changes in tendon-related research. Therefore, the authors suggest referring to the mentioned literature when searching for possible scoring systems.

Summary and conclusion

Tendinopathies are prevalent in orthopaedics and optimal therapies are still challenging since restoration of the special tendon tissue characteristics is rarely achieved. There is a strong need for research into enhanced therapeutic options. Histological evaluation of tendon is an essential component not only in research but also in diagnosis. Consideration for sample processing must take into account the properties of the sample in question. Embedding in paraffin-wax is most common and is the processing

technique of choice for soft-tissue samples. If the sample contains both soft and hard tissues such as calcifications/ossifications, cutting in paraffin-wax is not possible and plastic embedding in Technovit has to be chosen. Existing metal implants pose a special challenge. Here, embedding in Technovit is also mandatory and potential options for further processing are cutting and grinding of the sample or electrochemical dissolution of the implant.

There are different staining possibilities depending on the embedding medium. While paraffin-wax embedding enables all standard and specialised staining techniques, plastic-embedded samples require specific consideration. More complex protocols such as enzyme-based staining techniques or IHC are more challenging and special protocols are needed.

This review presents a compilation of the most common processing and staining techniques regarding tendinopathies, evaluation of their uses and disadvantages. Furthermore, a flow chart was provided for the processing of tendon tissue with different characteristics and a decision guide for common possible staining techniques regarding the different research foci of general overview, structure of tendon tissue and cells within tendon tissue to support optimal sample utilisation.

List of common stains

A list of common and useful staining techniques for the evaluation of tendons and enthesis is provided here. For each stain, basic knowledge, the general chemical content and colouring results are described while advantages and disadvantages have already been discussed. For each staining technique some example of references are given.

This list is not comprehensive but offers a summary of common pivotal techniques. The colours named for the specific structures derives both from established books of microscopical/histological techniques (*e.g.* Bancroft *et al.*, 2019), manuscripts (see respective stain) and the authors own experience. For further details or additional staining possibilities, refer to the mentioned literature.

Generally, stainings can be divided based on the underlying staining techniques and the following list is sorted accordingly.

Dye-based staining techniques

H&E – general cellular reactions

H&E belongs to the most common and therefore best-established dyes. Haematoxylin is processed to haemalum, which binds to basophilic structures especially in the cell nuclei. Eosin is a synthetic dye that stains acidophilic structures (also called eosinophilic), especially cytoplasmic proteins. Execution of H&E staining for paraffin-wax- and Technovit-embedded slices cut by microtome is similar, with staining duration for haemalum of up to 8 min and eosin of up to 5 min, while Technovit 7200-embedded ground sections have to be stained for up to 40 min with haemalum.

Example references: de Lima Santos *et al.*, 2020; Nakanishi *et al.*, 2019; Rashid *et al.*, 2020; Xu *et al.*, 2019.

Toluidine blue – bone tissue and cellular structures

Toluidine blue is a thiazine dye and also a very common standard staining method, being easy and quick to perform. Cell nuclei appear dark blue while the other tissues are stained blue to light blue depending on their predominant charge. Cytoplasm, aligned collagen (*e.g.* tendons) or non-aligned collagen (*e.g.* osteoid) show different shades of blue

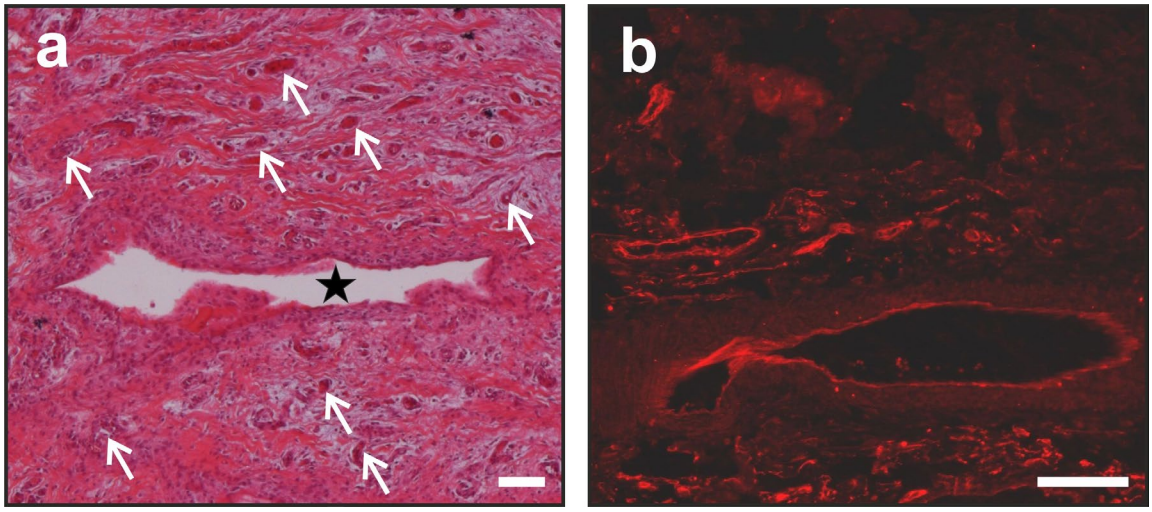

Fig. 11. Tendon sample of long part of muscle biceps brachii for depiction of vessels. (**a**,**b**) Scale bar: 100 μm. (**a**) Large vessel (black star) in the centre of the picture surrounded by numerous small vessels in the periphery (white arrows). (**b**) Similar part of the sample with immunohistochemical staining of the endothelial walls using fluorescence labelling. (**a**,**b**) Human tendon biopsy, part of biceps tendon of a patient with aseptic bursitis, embedding in Technovit 9100, microtome section, thickness 4 μm, (**a**) H&E, (**b**) anti-CD34-Cy3 labelled.

while mineralised bone tissue appears light blue to colourless. Furthermore, toluidine blue exhibits metachromatic properties, which means that cell and tissue parts display a colour different from the dye used. For example, granules of mastocytes, cartilage or early stages of wound healing areas are metachromatic red-violet following staining with toluidine blue.

Toluidine blue can be used for both paraffin-wax- and plastic-embedded samples. It can also penetrate well into the surface of the embedding medium so that removal of Technovit from ground sections is not necessary. Independent of the removal of the embedding medium, tissue staining duration is very short.

Example references: Bergholt *et al.*, 2019; Nakagaki *et al.*, 2013; Wang *et al.*, 2017; Yoshida *et al.*, 2016.

Safranin O-fast green – cartilage and bone structures

Safranin O is an alkaline azo dye, usually having two methyl groups. It stains tissue structures in different shades of red. Cell nuclei are coloured deep red, chondrocytes (as specific cell type) light red. The basic substance of cartilage is stained from red to pink/rose depending upon the GAG content.

This allows for a very differentiated evaluation of changes in cartilage structure. In combination with fast green, the cartilage structures can be strongly contrasted from the bone, since fast green does not stain the cartilage but the mineralised bone tissue as well as connective tissue intensely green. Dehydration following staining procedure has to be performed very carefully and only for a short time because the stain is very easily removed.

Example references: Kataoka *et al.*, 2018; Kataoka *et al.*, 2021; Mutsuzaki and Nakajima, 2020.

Masson-Goldner trichrome – different types of tissue

Masson-Goldner trichrome is a stepwise, multiple-dye coloration. It offers clear staining of nuclei and distinguishes between different types of tissues. Epithelium and muscles are well displayed in different shades of grey whereas collagenous structures, including bone, are in green. Usually, the first applied dye is iron haematoxylin, which stains cell nuclei in dark blue. The other dyes can be applied sequentially or together. The following dyes are used: xylidine ponceau, azophloxine, acid fuchsine, orange G and light green. The differentiation in acetic acid removes orange G at a slower rate out of erythrocytes than out of other tissues, leaving them clearly recognisable in bright orange. Since this staining enables a clear differentiation between several tissues of the musculoskeletal system, it is a favoured staining technique in orthopaedic histology. However, due to the amount of solutions applied, a more experienced technician should perform or supervise the procedure. The intensity of the different dyes depends on the turnaround time of the samples within the single solutions. While certain times are proposed, checking by microscope should be performed during the staining procedure to ensure favourable results.

Example references: Bi *et al.*, 2007; Schmalzl *et al.*, 2019; Wang *et al.*, 2017; Weiler *et al.*, 2002.

Picrosirius red – differentiation between muscles and tendon

Picrosirius red (derivate F3B or F3A) is present in a saturated aqueous solution of picric acid. Picrosirius red staining is used to detect collagen fibres. Muscles fibres, cytoplasm and tissue background appear yellow while the collagen fibres red. This red stain leads to an increase birefringence when it accumulates along the collagen fibres. Therefore, picrosirius red is often used in combination with polarised-light microscopy. This combination additionally allows type I and type III collagen fibres to be separated since they appear in different colours: the thicker type I collagen fibres are presented in yellow-orange while the thinner type III collagen fibres show a green double refraction.

Picrosirius red diffuses slowly into thicker tissue structures. Therefore, a staining time of 1 up to 2 h only leads to pale staining of non-collagen tissues. The staining protocol for paraffin-wax- and Technovit-embedded samples is nearly the same, with prolonged staining time in case of Technovit 9100. Independent of the embedding medium, checking by microscope of the staining result is advisable.

Example references: Blomgran *et al.*, 2017; Kataoka *et al.*, 2018; Nakagaki *et al.*, 2013; Ueda *et al.*, 2019; Zhang *et al.*, 2020.

von Kossa – mineralised/calcified tissue

Marlon Schneider recently published a comprehensive commentary on the von Kossa staining technique (Schneider, 2021). von Kossa staining is a two-step reaction with silver cations reacting firstly with calcium deposits, which are stained transiently in yellow. Secondly, the bound silver is reduced to black metallic silver by organic material in the presence of light (Schneider, 2021). While especially calcium-phosphate-rich tissue areas are stained deeply black, it has to be noted that this technique is unspecific since also chlorides, phosphates, sulphates, carbonates and fatty acids could react. It is also advisable that fixation solutions should not include calcium salts and use of metal instruments should be avoided (Mulisch *et al.*, 2015). The reactive chemicals of von Kossa staining are silver nitrate, pyrogallol and sodium thiosulphate. Execution of the staining procedure does not differ between paraffin-wax- and plastic-embedded samples.

Example references: Carvalho *et al.*, 2020; Limraksasin *et al.*, 2020; Schneider, 2021; Wu *et al.*, 2020; Zegyer *et al.*, 2020.

Alcian blue – extracellular matrix, connective tissue

Alcian blue as a phthalocyanine dye is cationic and water-soluble and stains acidic mucins and GAGs at

low pH values of 1.0 to 2.5. Therefore, *e.g.* hyaluronic acid or chondroitin sulphate are selectively stained in blue. Depending on the pH value, carboxyl and sulphate groups can be distinguished. Often, additional staining of cell nuclei is performed, *e.g.* with Nuclear Fast Red-aluminium sulphate solution, since they are not stained by alcian blue itself.

Alcian blue and safranin O are often used separately or in combination to increase their informative value. Depending on the tissue and the previous histological processing, alcian blue stains mainly GAGs whereas safranin O is more specific for proteoglycans. When both dyes are applied in combination, cell nuclei are stained in red by safranin O.

Example references: Ahlen *et al.*, 2014; Bedi *et al.*, 2009; Chard *et al.*, 1994; Kobayashi *et al.*, 2020; Zhang *et al.*, 2020.

Herovici – collagen with differentiation of mature/immature collagen

Herovici staining techniques constitute the use of several dyes, resulting in a polychromatic staining. It distinguishes between young collagen, which is stained in blue, and mature collagen, which is stained in pink to red (Teuscher *et al.*, 2019). As it includes numerous chemicals (coelestine blue iron alum solution, Nuclear Fast Red, metanil yellow, acetic acid, lithium carbonate, fuchsin-picric acid) the staining procedure should be performed by an experienced technician if solutions are prepared. Otherwise, there are staining kits available that provide the ready-to-use solutions (*e.g.* Staining Kit: HEROVICI for collagen differentiation; 18432, Morphisto GmbH, Germany). Beside collagen, stained structures are cytoplasm (yellow-green), muscles (yellow) and cell nuclei (black) (Teuscher *et al.*, 2019). Staining procedure is similar for paraffin-wax- and plastic-embedded samples.

Example references: Michel *et al.*, 2020; Pei *et al.*, 2015; Teuscher *et al.*, 2019.

Enzyme-based staining techniques

Chloroacetate esterase – neutrophil granulocytes

Enzyme-based staining techniques use already present tissue enzymes to split components of the substrate. For chloroacetate esterase staining, the substrate is naphthol AS-D chloroacetate. The enzyme liberates a free naphthol compound, which then couples by means of an azo coupling reaction to hexazonium pararosanillin forming strongly stained deposits at sites of enzyme activity. Chloroacetate esterase is used to detect neutrophil granulocytes. While this cell type shows a bright-red staining of the cytoplasm, monocytes also react, but with a paler staining result. Furthermore, mastocytes react strongly.

As the successful completion of the staining depends on a competent enzyme reaction, it is necessary to simultaneously stain control slides of known content *e.g.* spleen or bone marrow samples. On the other hand, a negative control should be performed where the substrate (naphthol AS-D chloroacetate) is left out. For all samples, the embedding medium has to be removed as described earlier. If the Technovit 9100-embedded slices contain bone tissue, decalcifying could be achieved by incubating with EDTA-containing buffer for 1 h. There are ready-to-use solutions available, *e.g.* Usedecalc® (decalcifying solution, Medite, Switzerland). While the staining procedure itself is not complicated, preparation of the staining solutions involved has to be performed carefully following the protocol. As usual for enzymatic reactions, the staining solution cannot be reused since the substrates are consumed.

Example references: Wichelhaus *et al.*, 2016; Willbold *et al.*, 2020.

Immunohistochemical staining techniques

CD68 – detection of macrophages

CD68 is a transmembrane glycoprotein commonly present in various cells of the macrophage lineage. Macrophages can be distinguished in pro-inflammatory (M1) and more anti-inflammatory (M2) macrophages and further subtypes, which are the topic of several research papers and reviews (Dakin *et al.*, 2012; Koh and DiPietro, 2011; Sunwoo *et al.*, 2020; Xu *et al.*, 2019; Yunna *et al.*, 2020). As a first step to distinguish between these types it is important to determine the number of macrophages as well as multinucleated phagocytes present by respective labelling. Anti-CD68 is available from numerous companies for numerous species and in combination with different labelling systems.

For the samples presented in the present review, a mouse anti-CD68 primary antibody was used, purchased from either abcam (ab955, abcam, Cambridge, UK; dilution 1:100) or OriGene (TA354352, OriGene EU, Herford, Germany; dilution 1:100). The secondary antibody derived from goat (goat anti-mouse) and was purchased from Dianova (GtxMu-003-FBIO, Dianova, Hamburg, Germany; dilution 1:500) and labelled with biotin. Streptavidin-Cy3 (016-160-084, Dianova, Hamburg, Germany; 2 μg/mL) was used as detection system. After removal of paraffin-wax, antigen retrieval was achieved by boiling in citrate buffer for 20 min. Non-specific binding of the secondary antibody was avoided by blocking with 2 % normal goat serum before incubation with the primary antibody. All rinsing steps were performed in TBS.

Example references: Scott *et al.*, 2008; Shaw *et al.*, 2007; Sugg *et al.*, 2014.

CD34 – detection of endothelial cells

CD34 is also a transmembrane glycoprotein, which is present with highest densities on haematopoietic progenitor cells and leukocytes (stage-specific) as well as on capillary endothelial cells.

The antibody is available from different distributors and out of different species. After blocking the endogenous bonding sites with 2 %

normal goat serum, a mouse anti-CD34 from Boster (PA1334, Boster Biological Technology, Pleasanton, USA; dilution 1:250) was used as primary antibody for paraffin-wax-embedded samples (ovine and human). Secondary antibody and labelling system corresponded to the anti-CD68 protocol [secondary antibody: goat anti-mouse (GtxMu-003-FBIO, Dianova, Hamburg, Germany; dilution 1:500), labelled with biotin, detected using streptavidin-Cy3 (016-160-084, Dianova, Hamburg, Germany; 2 µg/mL)]. Antigen retrieval was performed after boiling in citrate buffer. Citrate buffer was prepared using citric acid, sodium citrate and distilled water. All rinsing steps were carried out using TBS.

Exemplary references: Handa *et al.*, 2003; Zabrzynski *et al.*, 2018; Zabrzynski *et al.*, 2020; Zhang *et al.*, 2016.

Other techniques

Polarised-light microscopy

Structural components of tissue can be easily studied by polarised-light microscopy. It only requires a specialised microscope. Anisotropic objects can be detected because their structure differently influences the rotation of the light they transmit. The original unpolarised light beam is converted so as to be polarised in a single direction by passing it through a polarising filter – normally termed the polariser - before passing through the specimen. After being transmitted through the specimen, the light is passed through a second polarising filter - the analyser – whose rotational position can be adjusted. When the two polarising filters are rotated at 90° to each other, no light will pass through (the field of view will be black) – except where parts of the specimen exhibit birefringence (e.g. oriented fibres or crystals), which are detected as bright parts of the image.

Example references: Liu *et al.*, 2021; Lopez De Padilla *et al.*, 2021; Tempfer *et al.*, 2015; Tempfer *et al.*, 2018.

Acknowledgements

The authors thank Diana Strauch, Stefanie Rausch, Mattias Reebmann and Maike Haupt for excellent laboratory technical work and support and Yvonne Noll for application of ethical approval for human-derived samples. Furthermore, the authors thank the DFG for funding WE4262/6-2 within the framework of FOR 2180.

References

Ackermann PW, Li J, Lundeberg T, Kreicbergs A (2003) Neuronal plasticity in relation to nociception and healing of rat Achilles tendon. J Orthop Res **21**: 432-441.

Åhlén M, Lidén M, Movin T, Papadogiannakis N, Rostgård-Christensen L, Kartus J (2014) Histological evaluation of regenerated semitendinosus tendon a minimum of 6 years after harvest for anterior cruciate ligament reconstruction. Orthop J Sports Med **2**: 2325967114550274. DOI: 10.1177/2325967114550274.

Alim MA, Peterson M, Pejler G (2020) Do mast cells have a role in tendon healing and inflammation? Cells **9**: 1134. DOI: 10.3390/cells9051134.

Al-Maawi S, Vorakulpipat C, Orlowska A, Zrnc TA, Sader RA, Kirkpatrick CJ, Ghanaati S (2018) *In vivo* implantation of a bovine-derived collagen membrane leads to changes in the physiological cellular pattern of wound healing by the induction of multinucleated giant cells: an adverse reaction? Front Bioeng Biotechnol **6**: 104. DOI: 10.3389/fbioe.2018.00104.

Andersson G, Danielson P, Alfredson H, Forsgren S (2007) Nerve-related characteristics of ventral paratendinous tissue in chronic Achilles tendinosis. Knee Surg Sports Traumatol Arthrosc **15**: 1272-1279.

Barros MH, Hauck F, Dreyer JH, Kempkes B, Niedobitek G (2013) Macrophage polarisation: an immunohistochemical approach for identifying M1 and M2 macrophages. PLoS One **8**: e80908. DOI: 10.1371/journal.pone.0080908.

Bedi A, Kawamura S, Ying L, Rodeo SA (2009) Differences in tendon graft healing between the intra-articular and extra-articular ends of a bone tunnel. HSS J **5**: 51-57.

Benjamin M, McGonagle D (2001) The anatomical basis for disease localisation in seronegative spondyloarthropathy at entheses and related sites. J Anat **199**: 503-526.

Benjamin M, McGonagle D (2007) Histopathologic changes at "synovio–entheseal complexes" suggesting a novel mechanism for synovitis in osteoarthritis and spondylarthritis. Arthritis Rheum **56**: 3601-3609.

Bergholt NL, Lysdahl H, Lind M, Foldager CB (2019) A standardized method of applying toluidine blue metachromatic staining for assessment of chondrogenesis. Cartilage **10**: 370-374.

Bi Y, Ehirchiou D, Kilts TM, Inkson CA, Embree MC, Sonoyama W, Li L, Leet AI, Seo BM, Zhang L, Shi S, Young MF (2007) Identification of tendon stem/progenitor cells and the role of the extracellular matrix in their niche. Nat Med **13**: 1219-1227.

Blomgran P, Hammerman M, Aspenberg P (2017) Systemic corticosteroids improve tendon healing when given after the early inflammatory phase. Sci Rep **7**: 12468. DOI: 10.1038/s41598-017-12657-0.

Bridgewood C, Sharif K, Freeston J, Saleem B, Russell T, Watad A, Khan A, Loughenbury P, Rao A, Wittmann M, McGonagle D (2021) Regulation of entheseal IL-23 expression by IL-4 and IL-13 as an explanation for arthropathy development under dupilumab therapy. Rheumatology (Oxford) **60**: 2461-2466.

Brooks CH, Revell WJ, Heatley FW (1992) A quantitative histological study of the vascularity of the rotator cuff tendon. J Bone Joint Surg Br **74**: 151-153.

Brown C, Sekhavati F, Cardenes R, Windmueller C, Dacosta K, Rodriguez-Canales J, Steele KE (2019) CTLA-4 immunohistochemistry and quantitative image analysis for profiling of human cancers. J Histochem Cytochem **67**: 901-918.

Bystrom J, Evans I, Newson J, Stables M, Toor I, van Rooijen N, Crawford M, Colville-Nash P, Farrow S, Gilroy DW (2008) Resolution-phase macrophages possess a unique inflammatory phenotype that is controlled by cAMP. Blood **112**: 4117-4127.

Campbell TM, Lapner P, Dilworth FJ, Sheikh MA, Laneuville O, Uhthoff H, Trudel G (2019) Tendon contains more stem cells than bone at the rotator cuff repair site. J Shoulder Elbow Surg **28**: 1779-1787.

Carvalho AAM, Moura FBR, Nogueira PAS, Gonçalves AMN, Araújo FA, Zanon RG, Tomiosso TC (2020) Swimming exercise changed the collagen synthesis and calcification in calcaneal tendons of mice. An Acad Bras Cienc **92**: e20181127. DOI: 10.1590/0001-3765202020181127.

Chard MD, Cawston TE, Riley GP, Gresham GA, Hazleman BL (1994) Rotator cuff degeneration and lateral epicondylitis: a comparative histological study. Ann Rheum Dis **53**: 30-34.

Chard MD, Hazleman R, Hazleman BL, King RH, Reiss BB (1991) Shoulder disorders in the elderly: a community survey. Arthritis Rheum **34**: 766-769.

Chisari E, Rehak L, Khan WS, Maffulli N (2020) The role of the immune system in tendon healing: a systematic review. Br Med Bull **133**: 49-64.

Claudepierre P, Voisin MC (2005) The entheses: histology, pathology, and pathophysiology. Joint Bone Spine **72**: 32-37.

Connizzo BK, Yannascoli SM, Soslowsky LJ (2013) Structure-function relationships of postnatal tendon development: a parallel to healing. Matrix Biol **32**: 106-116.

Courtoy GE, Leclercq I, Froidure A, Schiano G, Morelle J, Devuyst O, Huaux F, Bouzin C (2020) Digital image analysis of picrosirius red staining: a robust method for multi-organ fibrosis quantification and characterization. Biomolecules **10**: 1585. DOI: 10.3390/biom10111585.

da Silva EZ, Jamur MC, Oliver C (2014) Mast cell function: a new vision of an old cell. J Histochem Cytochem **62**: 698-738.

Dai G, Li Y, Liu J, Zhang C, Chen M, Lu P, Rui Y (2020) Higher BMP expression in tendon stem/progenitor cells contributes to the increased heterotopic ossification in Achilles tendon with aging. Front Cell Dev Biol **8**: 570605. DOI: 10.3389/fcell.2020.570605.

Dakin SG, Werling D, Hibbert A, Abayasekara DR, Young NJ, Smith RK, Dudhia J (2012) Macrophage sub-populations and the lipoxin A4 receptor implicate active inflammation during equine tendon repair. PLoS One **7**: e32333. DOI: 10.1371/journal.pone.0032333.

de Lima Santos A, da Silva CG, de Sá Barreto LS, Leite KRM, Tamaoki MJS, Ferreira LM, de Almeida FG, Faloppa F (2020) A new decellularized tendon scaffold for rotator cuff tears - evaluation in rabbits. BMC Musculoskelet Disord **21**: 689. DOI: 10.1186/s12891-020-03680-w.

Donath K, Breuner G (1982) A method for the study of undecalcified bones and teeth with attached soft tissues. The Säge-Schliff (sawing and grinding) technique. J Oral Pathol **11**: 318-326.

Fecher-Trost C, Lux F, Busch K, Raza A, Winter M, Hielscher F, Belkacemi T, van der Eerden B, Boehm U, Freichel M, Weissgerber P (2019) Maternal transient receptor potential vanilloid 6 (TRPV6) is involved in offspring bone development. J Bone Min Res **34**: 699-710.

Florit D, Pedret C, Casals M, Malliaras P, Sugimoto D, Rodas G (2019) Incidence of tendinopathy in team sports in a multidisciplinary sports club over 8 seasons. J Sports Sci Med **18**: 780-788.

Font Tellado S, Balmayor ER, Van Griensven M (2015) Strategies to engineer tendon/ligament-to-bone interface: biomaterials, cells and growth factors. Adv Drug Deliv Rev **94**: 126-140.

Fu SC, Rolf C, Cheuk YC, Lui PP, Chan KM (2010) Deciphering the pathogenesis of tendinopathy: a three-stages process. Sports Med Arthrosc Rehabil Ther Technol **2**: 30-30.

Galatz LM, Sandell LJ, Rothermich SY, Das R, Mastny A, Havlioglu N, Silva MJ, Thomopoulos S (2006) Characteristics of the rat supraspinatus tendon during tendon-to-bone healing after acute injury. J Orthop Res **24**: 541-550.

Ge Z, Tang H, Chen W, Wang Y, Yuan C, Tao X, Zhou B, Tang K (2020) Downregulation of type I collagen expression in the Achilles tendon by dexamethasone: a controlled laboratory study. J Orthop Surg Res **15**: 70. DOI: 10.1186/s13018-020-01602-z.

Gniesmer S, Brehm R, Hoffmann A, de Cassan D, Menzel H, Hoheisel AL, Glasmacher B, Willbold E, Reifenrath J, Wellmann M, Ludwig N, Tavassol F, Zimmerer R, Gellrich NC, Kampmann A (2019) *In vivo* analysis of vascularization and biocompatibility of electrospun polycaprolactone fibre mats in the rat femur chamber. J Tissue Eng Regen Med **13**: 1190-1202.

Gordon S, Hamann J, Lin HH, Stacey M (2011) F4/80 and the related adhesion-GPCRs. Eur J Immunol **41**: 2472-2476.

Handa A, Gotoh M, Hamada K, Yanagisawa K, Yamazaki H, Nakamura M, Ueyama Y, Mochida J, Fukuda H (2003) Vascular endothelial growth factor 121 and 165 in the subacromial bursa are involved in shoulder joint contracture in type II diabetics with rotator cuff disease. J Orthop Res **21**: 1138-1144.

Heinemeier KM, Schjerling P, Øhlenschlæger TF, Eismark C, Olsen J, Kjær M (2018) Carbon-14 bomb pulse dating shows that tendinopathy is preceded by years of abnormally high collagen turnover. FASEB J **32**: 4763-4775.

Hopkins C, Fu SC, Chua E, Hu X, Rolf C, Mattila VM, Qin L, Yung PS, Chan KM (2016) Critical review on the socio-economic impact of tendinopathy. Asia Pac J Sports Med Arthrosc Rehabil Technol **4**: 9-20.

Huang Y, de Boer WB, Adams LA, MacQuillan G, Rossi E, Rigby P, Raftopoulos SC, Bulsara M, Jeffrey GP (2013) Image analysis of liver collagen using sirius red is more accurate and correlates better with serum fibrosis markers than trichrome. Liver Int **33**: 1249-1256.

Järvinen TA (2020) Neovascularisation in tendinopathy: from eradication to stabilisation? Br J Sports Med **54**: 1-2.

Jomaa G, Kwan CK, Fu SC, Ling SK, Chan KM, Yung PS, Rolf C (2020) A systematic review of inflammatory cells and markers in human tendinopathy. BMC Musculoskelet Disord **21**: 78. DOI: 10.1186/s12891-020-3094-y.

Junqueira LC, Bignolas G, Brentani RR (1979) Picrosirius staining plus polarization microscopy, a specific method for collagen detection in tissue sections. Histochem J **11**: 447-455.

Kataoka T, Kokubu T, Muto T, Mifune Y, Inui A, Sakata R, Nishimoto H, Harada Y, Takase F, Ueda Y, Kurosawa T, Yamaura K, Kuroda R (2018) Rotator cuff tear healing process with graft augmentation of fascia lata in a rabbit model. J Orthop Surg Res **13**: 200-204.

Kataoka T, Mifune Y, Inui A, Nishimoto H, Kurosawa T, Yamaura K, Mukohara S, Matsushita T, Niikura T, Tabata Y, Kuroda R (2021) Combined therapy of platelet-rich plasma and basic fibroblast growth factor using gelatin-hydrogel sheet for rotator cuff healing in rat models. J Orthop Surg Res **16**: 605-611.

Kawamoto T (2003) Use of a new adhesive film for the preparation of multi-purpose fresh-frozen sections from hard tissues, whole-animals, insects and plants. Arch Histol Cytol **66**: 123-143.

Kawamoto T, Kawamoto K (2020) Preparation of thin frozen sections from nonfixed and undecalcified hard tissues using Kawamoto's film method. In: Skeletal Development and Repair. Methods in Molecular Biology. Editor: Hilton M. Vol 1130. pp: 259-281. Humana Press, Totowa, NJ, USA.

Kobayashi Y, Saita Y, Takaku T, Yokomizo T, Nishio H, Ikeda H, Takazawa Y, Nagao M, Kaneko K, Komatsu N (2020) Platelet-rich plasma (PRP) accelerates murine patellar tendon healing through enhancement of angiogenesis and collagen synthesis. J Exp Orthop **7**: 49-51.

Koh TJ, DiPietro LA (2011) Inflammation and wound healing: the role of the macrophage. Expert Rev Mol Med **13**: e23. DOI: 10.1017/S1462399411001943.

Krystel-Whittemore M, Dileepan KN, Wood JG (2016) Mast cell: a multi-functional master cell. Front Immunol **6**: 620. DOI: 10.3389/fimmu.2015.00620.

Labow RS, Meek E, Santerre JP (2001) Neutrophil-mediated biodegradation of medical implant materials. J Cell Physiol **186**: 95-103.

Laschke MW, Harder Y, Amon M, Martin I, Farhadi J, Ring A, Torio-Padron N, Schramm R, Rücker M, Junker D, Häufel JM, Carvalho C, Heberer M, Germann G, Vollmar B, Menger MD (2006) Angiogenesis in tissue engineering: breathing life into constructed tissue substitutes. Tissue Eng **12**: 2093-2104.

Lattouf R, Younes R, Lutomski D, Naaman N, Godeau G, Senni K, Changotade S (2014) Picrosirius red staining: a useful tool to appraise collagen networks in normal and pathological tissues. J Histochem Cytochem **62**: 751-758.

Lawrence RL, Moutzouros V, Bey MJ (2019) Asymptomatic rotator cuff tears. JBJS Rev **7**: e9. DOI: 10.2106/JBJS.RVW.18.00149.

Le BT, Wu XL, Lam PH, Murrell GA (2014) Factors predicting rotator cuff retears: an analysis of 1000 consecutive rotator cuff repairs. Am J Sports Med **42**: 1134-1142.

Limraksasin P, Okawa H, Zhang M, Kondo T, Osathanon T, Pavasant P, Egusa H (2020) Size-optimized microspace culture facilitates differentiation of mouse induced pluripotent stem cells into osteoid-rich bone constructs. Stem Cells Int **2020**: 7082679. DOI: 10.1155/2020/7082679

Liu J, Xu MY, Wu J, Zhang H, Yang L, Lun DX, Hu YC, Liu B (2021) Picrosirius-polarization method for collagen fiber detection in tendons: a mini-review. Orthop Surg **13**: 701-707.

Longo UG, Franceschi F, Ruzzini L, Rabitti C, Morini S, Maffulli N, Denaro V (2008) Histopathology of the supraspinatus tendon in rotator cuff tears. Am J Sports Med **36**: 533-538.

Lopéz De Padilla CM, Coenen MJ, Tovar A, De la Vega, R E, Evans CH, Müller SA (2021) Picrosirius red staining: revisiting its application to the qualitative and quantitative assessment of collagen type I and type III in tendon. J Histochem Cytochem **69**: 633-643.

Loppini M, Longo UG, Niccoli G, Khan WS, Maffulli N, Denaro V (2015) Histopathological scores for tissue-engineered, repaired and degenerated tendon: a systematic review of the literature. Curr Stem Cell Res Ther **10**: 43-55.

Maffulli N, Barrass V, Ewen SW (2000) Light microscopic histology of Achilles tendon ruptures. A comparison with unruptured tendons. Am J Sports Med **28**: 857-863.

Mantovani A, Biswas SK, Galdiero MR, Sica A, Locati M (2013) Macrophage plasticity and polarization in tissue repair and remodelling. J Pathol **229**: 176-185.

Mariani E, Lisignoli G, Borzi RM, Pulsatelli L (2019) Biomaterials: foreign bodies or tuners for the immune response? Int J Mol Sci **20**: 636. DOI: 10.3390/ijms20030636.

Marinovich R, Soenjaya Y, Wallace GQ, Zuskov A, Dunkman A, Foster BL, Ao M, Bartman K, Lam V, Rizkalla A, Beier F, Somerman MJ, Holdsworth DW, Soslowsky LJ, Lagugné-Labarthet F, Goldberg HA (2016) The role of bone sialoprotein in the tendon-bone insertion. Matrix Biol **52-54**: 325-338.

Matthews TJ, Hand GC, Rees JL, Athanasou NA, Carr AJ (2006) Pathology of the torn rotator cuff tendon. Reduction in potential for repair as tear size increases. J Bone Joint Surg Br **88**: 489-495.

Mauro A, Russo V, Di Marcantonio L, Berardinelli P, Martelli A, Muttini A, Mattioli M, Barboni B (2016) M1 and M2 macrophage recruitment during tendon regeneration induced by amniotic epithelial cell allotransplantation in ovine. Res Vet Sci **105**: 92-102.

Mescher AL (2017) Macrophages and fibroblasts during inflammation and tissue repair in models of organ regeneration. Regeneration **4**: 39-53.

Michel PA, Kronenberg D, Neu G, Stolberg-Stolberg J, Frank A, Pap T, Langer M, Fehr M, Raschke MJ, Stange R (2020) Microsurgical reconstruction affects the outcome in a translational mouse model for Achilles tendon healing. J Orthop Translat **24**: 1-11.

Miranda H, Viikari-Juntura E, Heistaro S, Heliövaara M, Riihimäki H (2005) A population study on differences in the determinants of a specific shoulder disorder *versus* nonspecific shoulder pain without clinical findings. Am J Epidemiol **161**: 847-855.

Moffat KL, Sun WH, Pena PE, Chahine NO, Doty SB, Ateshian GA, Hung CT, Lu HH (2008) Characterization of the structure-function relationship at the ligament-to-bone interface. Proc Natl Acad Sci U S A **105**: 7947-7952.

Mulisch M, Welsch U, Romeis B, Aescht E (2015) Romeis Mikroskopische Technik, 19. Auflage ed. Springer Spektrum, Berlin.

Mutsuzaki H, Nakajima H (2020) Differences in the development of fibrocartilage layers in the quadriceps tendon and patellar tendon insertions in rabbits: a quantitative study. Orthop J Sports Med **8**: 2325967120966418. DOI: 10.1177/2325967120966418.

Nakagaki WR, Tomiosso TC, Pimentel ER, Camilli JA (2013) Mechanical and morphological aspects of the calcaneal tendon of mdx mice at 21 days of age. Anat Rec (Hoboken) **296**: 1546-1551.

Nakanishi Y, Okada T, Takeuchi N, Kozono N, Senju T, Nakayama K, Nakashima Y (2019) Histological evaluation of tendon formation using a scaffold-free three-dimensional-bioprinted construct of human dermal fibroblasts under *in vitro* static tensile culture. Regen Ther **11**: 47-55.

Pei M, Li J, McConda DB, Wen S, Clovis NB, Danley SS (2015) A comparison of tissue engineering based repair of calvarial defects using adipose stem cells from normal and osteoporotic rats. Bone **78**: 1-10.

Plecko M, Sievert C, Andermatt D, Frigg R, Kronen P, Klein K, Stübinger S, Nuss K, Bürki A, Ferguson S, Stoeckle U, von Rechenberg B (2012) Osseointegration and biocompatibility of different metal implants - a comparative experimental investigation in sheep. BMC Musculoskelet Disord **13**: 32. DOI: 10.1186/1471-2474-13-32.

Podszun MC, Chung JY, Ylaya K, Kleiner DE, Hewitt SM, Rotman Y (2020) 4-HNE Immunohistochemistry and image analysis for detection of lipid peroxidation in human liver samples using vitamin E treatment in NAFLD as a proof of concept. J Histochem Cytochem **68**: 635-643.

Rammelt S, Corbeil D, Manthey S, Zwipp H, Hanisch U (2007) Immunohistochemical *in situ* characterization of orthopedic implants on polymethyl metacrylate embedded cutting and grinding sections. J Biomed Mater Res A **83**: 313-322.

Rashid M, Dudhia J, Dakin SG, Snelling S, Lach A, De Godoy R, Mouthuy PA, Smith R, Morrey M, Carr AJ (2020) Histological evaluation of cellular response to a multifilament electrospun suture for tendon repair. PLoS One **15**: e0234982. DOI: 10.1371/journal.pone.0234982.

Rigueur D, Lyons KM (2014) Whole-mount skeletal staining. Methods Mol Biol **1130**: 113-121.

Roßbach BP, Gülecyüz MF, Kempfert L, Pietschmann MF, Ullamann T, Ficklscherer A, Niethammer TR, Zhang A, Klar RM, Müller PE (2020) Rotator Cuff repair with autologous tenocytes and biodegradable collagen scaffold: a histological and biomechanical study in sheep. Am J Sports Med **48**: 450-459.

Salles MB, König B Jr, Allegrini S Jr, Yoshimoto M, Martins MT, Coelho PG (2011) Identification of the nuclear factor kappa-beta (NF-kB) in cortical of mice Wistar using Technovit 7200 VCR®. Med Oral Patol Oral Cir Bucal **16**: e124-131.

Schmalzl J, Plumhoff P, Gilbert F, Gohlke F, Konrads C, Brunner U, Jakob F, Ebert R, Steinert AF (2019) The inflamed biceps tendon as a pain generator in the shoulder: a histological and biomolecular analysis. J Orthop Surg (Hong Kong) **27**: 2309499018820349. DOI: 10.1177/2309499018820349.

Schneider MR (2021) Von Kossa and his staining technique. Histochem Cell Biol **156**: 523-526.

Scott A, Backman LJ, Speed C (2015) Tendinopathy: update on pathophysiology. J Orthop Sports Phys Ther **45**: 833-841.

Scott A, Lian O, Bahr R, Hart DA, Duronio V, Khan KM (2008) Increased mast cell numbers in human patellar tendinosis: correlation with symptom duration and vascular hyperplasia. Br J Sports Med **42**: 753-757.

Shapiro E, Grande D, Drakos M (2015) Biologics in Achilles tendon healing and repair: a review. Curr Rev Musculoskelet Med **8**: 9-17.

Shaw HM, Benjamin M (2007) Structure-function relationships of entheses in relation to mechanical load and exercise. Scand J Med Sci Sports **17**: 303-315.

Shaw HM, Santer RM, Watson AH, Benjamin M (2007) Adipose tissue at entheses: the innervation and cell composition of the retromalleolar fat pad associated with the rat Achilles tendon. J Anat **211**: 436-443.

Shi Z, Zhang Y, Wang Q, Jiang D (2019) MFG-E8 regulates inflammation and apoptosis in tendon healing, and promotes tendon repair: a histological and biochemical evaluation. IUBMB Life **71**: 1986-1993.

Shields VDC, Heinbockel T (2019) Introductory chapter: histological microtechniques. In: Histology. IntechOpen. DOI: 10.5772/intechopen.75080.

Sobhani S, Dekker R, Postema K, Dijkstra PU (2013) Epidemiology of ankle and foot overuse injuries in sports: a systematic review. Scand J Med Sci Sports **23**: 669-686.

Sugg KB, Lubardic J, Gumucio JP, Mendias CL (2014) Changes in macrophage phenotype and induction of epithelial-to-mesenchymal transition genes following acute Achilles tenotomy and repair. J Orthop Res **32**: 944-951.

Sunwoo JY, Eliasberg CD, Carballo CB, Rodeo SA (2020) The role of the macrophage in tendinopathy and tendon healing. J Orthop Res **38**: 1666-1675.

Suvarna KS, Bancroft JD, Layton C (2018) Bancroft's theory and practice of histological techniques. Elsevier.

Svensson RB, Herchenhan A, Starborg T, Larsen M, Kadler KE, Qvortrup K, Magnusson SP (2017) Evidence of structurally continuous collagen fibrils in tendons. Acta Biomater **50**: 293-301.

Tajika T, Kobayashi T, Yamamoto A, Kaneko T, Takagishi K (2014) Prevalence and risk factors of lateral epicondylitis in a mountain village in Japan. J Orthop Surg (Hong Kong) **22**: 240-243.

Tempfer H, Kaser-Eichberger A, Korntner S, Lehner C, Kunkel N, Traweger A, Trost A, Strohmaier C, Bogner B, Runge C, Bruckner D, Krefft K, Heindl LM, Reitsamer HA, Schrodl F (2015) Presence of lymphatics in a rat tendon lesion model. Histochem Cell Biol **143**: 411-419.

Tempfer H, Kaser-Eichberger A, Lehner C, Gehwolf R, Korntner S, Kunkel N, Wagner A, Gruetz M, Heindl LM, Schroedl F, Traweger A (2018) Bevacizumab improves Achilles tendon repair in a rat model. Cell Physiol Biochem **46**: 1148-1158.

Terada T (2012) Giant cell tumor of the tendon sheath composed largely of epithelioid histiocytes. Int J Clin Exp Pathol **5**: 374-376.

Teuscher AC, Statzer C, Pantasis S, Bordoli MR, Ewald CY (2019) Assessing collagen deposition during aging in mammalian tissue and in *Caenorhabditis elegans*. Methods Mol Biol **1944**: 169-188.

Thomopoulos S, Parks WC, Rifkin DB, Derwin KA (2015) Mechanisms of tendon injury and repair. J Orthop Res **33**: 832-839.

Thorpe CT, Birch HL, Clegg PD, Screen HR (2013) The role of the non-collagenous matrix in tendon function. Int J Exp Pathol **94**: 248-259.

Titan A, Andarawis-Puri N (2016) Tendinopathy: investigating the intersection of clinical and animal research to identify progress and hurdles in the field. JBJS Rev **4**: 01874474-201610000-00004. DOI: 10.2106/JBJS.RVW.15.00088.

Tsang AS, Dart AJ, Biasutti SA, Jeffcott LB, Smith MM, Little CB (2019) Effects of tendon injury on uninjured regional tendons in the distal limb: an *in-vivo* study using an ovine tendinopathy model. PLoS One **14**: e0215830. DOI: 10.1371/journal.pone.0215830.

Turunen MJ, Khayyeri H, Guizar-Sicairos M, Isaksson H (2017) Effects of tissue fixation and dehydration on tendon collagen nanostructure. J Struct Biol **199**: 209-215.

Ueda Y, Inui A, Mifune Y, Takase F, Kataoka T, Kurosawa T, Yamaura K, Kokubu T, Kuroda R (2019) Molecular changes to tendons after collagenase-induced acute tendon injury in a senescence-accelerated mouse model. BMC Musculoskelet Disord **20**: 120. DOI: 10.1186/s12891-019-2488-1.

Vitale MA, Vitale MG, Zivin JG, Braman JP, Bigliani LU, Flatow EL (2007) Rotator cuff repair: an analysis of utility scores and cost-effectiveness. J Shoulder Elbow Surg **16**: 181-187.

Wang R, Xu B, Xu HG (2017) Up-regulation of TGF-beta promotes tendon-to-bone healing after anterior cruciate ligament reconstruction using bone marrow-derived mesenchymal stem cells through the TGF-beta/MAPK signaling pathway in a New Zealand white rabbit model. Cell Physiol Biochem **41**: 213-226.

Ward JM, Rehg JE (2014) Rodent immunohistochemistry: pitfalls and troubleshooting. Vet Pathol **51**: 88-101.

Weiler A, Hoffmann RF, Bail HJ, Rehm O, Südkamp NP (2002) Tendon healing in a bone tunnel. Part II: histologic analysis after biodegradable interference fit fixation in a model of anterior cruciate ligament reconstruction in sheep. Arthroscopy **18**: 124-135.

Wichelhaus A, Beyersdoerfer ST, Vollmar B, Mittlmeier T, Gierer P (2016) Four-strand core suture improves flexor tendon repair compared to two-strand technique in a rabbit model. Biomed Res Int 2016: 4063137. DOI: 10.1155/2016/4063137.

Willbold E, Reebmann M, Jeffries R, Witte F (2013) Electrochemical removal of metallic implants from Technovit 9100 New embedded hard and soft tissues prior to histological sectioning. Histochem Cell Biol **140**: 585-593.

Willbold E, Wellmann M, Welke B, Angrisani N, Gniesmer S, Kampmann A, Hoffmann A, de Cassan D, Menzel H, Hoheisel AL, Glasmacher B, Reifenrath J (2020) Possibilities and limitations of electrospun chitosan-coated polycaprolactone grafts for rotator cuff tear repair. J Tissue Eng Regen Med **14**: 186-197.

Willbold E, Witte F (2010) Histology and research at the hard tissue-implant interface using Technovit 9100 New embedding technique. Acta Biomater **6**: 4447-4455.

Wu CY, Martel J, Young JD (2020) Ectopic calcification and formation of mineralo-organic particles in arteries of diabetic subjects. Sci Rep **10**: 8545. DOI: 10.1038/s41598-020-65276-7.

Xu HT, Lee CW, Li MY, Wang YF, Yung PS, Lee OK (2019) The shift in macrophages polarisation after tendon injury: a systematic review. J Orthop Translat **21**: 24-34.

Xu T, Bai J, Xu M, Yu B, Lin J, Guo X, Liu Y, Zhang D, Yan K, Hu D, Hao Y, Geng D (2019) Relaxin inhibits

patellar tendon healing in rats: a histological and biochemical evaluation. BMC Musculoskelet Disord **20**: 349. DOI: 10.1186/s12891-019-2729-3.

Xu Y, Bonar F, Murrell GA (2011) Neoinnervation in rotator cuff tendinopathy. Sports Med Arthrosc Rev **19**: 354-359.

Yin N, Zhu L, Ding L, Yuan J, Du L, Pan M, Xue F, Xiao H (2019) MiR-135-5p promotes osteoblast differentiation by targeting HIF1AN in MC3T3-E1 cells. Cell Mol Biol Lett **24**: 51. DOI: 10.1186/s11658-019-0177-6.

Yoshida R, Alaee F, Dyrna F, Kronenberg MS, Maye P, Kalajzic I, Rowe DW, Mazzocca AD, Dyment NA (2016) Murine supraspinatus tendon injury model to identify the cellular origins of rotator cuff healing. Connect Tissue Res **57**: 507-515.

Yunna C, Mengru H, Lei W, Weidong C (2020) Macrophage M1/M2 polarization. Eur J Pharmacol **877**: 173090. DOI: 10.1016/j.ejphar.2020.173090.

Zabrzynski J, Gagat M, Paczesny L, Grzanka D, Huri G (2020) Correlation between smoking and neovascularization in biceps tendinopathy: a functional preoperative and immunohistochemical study. Ther Adv Chronic Dis **11**: 2040622320956418. DOI: 10.1177/2040622320956418.

Zabrzyński J, Paczesny L, Łapaj Ł, Grzanka D, Szukalski J (2018) Process of neovascularisation compared with pain intensity in tendinopathy of the long head of the biceps brachii tendon associated with concomitant shoulder disorders, after arthroscopic treatment. Microscopic evaluation supported by immunohistochemical. Folia Morphol (Warsz) **77**: 378-385.

Zegyer EAK, Khuzaee BAA, Badri AMA (2020) Detection of esophageal and glandular stomach calcification in cow (*Bos taurus*). Vet World **13**: 1153-1158.

Zhang L, Jiang K, Chai H, Zhou M, Bai J (2016) A comparative animal study of tendon grafts healing after remnant-preserving versus conventional anterior cruciate ligament reconstruction. Med Sci Monit **22**: 3426-3437.

Zhang Y, Deng XH, Lebaschi AH, Wada S, Carballo CB, Croen B, Ying L, Rodeo SA (2020) Expression of alarmins in a murine rotator cuff tendinopathy model. J Orthop Res **38**: 2513-2520.

Web References

1. www.section-lab.jp [27-04-2022]

2. http://kromat.hu/UserFiles/files/patologia/Dako_IHC_metodikai_k%C3%A9zik%C3%B6nyv_I.pdf [27-04-2022]

Discussion with Reviewers

Andreas Traweger: As outlined in the review article, there are several scoring systems available. In the authors' opinion, which are the most important characteristics that need to be semi-quantitatively evaluated and yield the most robust results? Do you believe AI-based histology/pathology can help to yield more objective results and, even more importantly, allow for a better comparison between study outcomes?

Authors: Evaluation depends often on the specific point of view. Parts of our studies concentrate on integration of tendon replacements and a functionally sufficient tendon-to-bone fixation comparable to the original enthesis. In these cases, structural aspects might be most important due to their relevance to the success of refixation. As an associated part, cells, as marker of inflammation and poor/good integration of tendon replacements, are also crucial to assess. If the applied placeholder induces inflammation or adverse cellular effects, the needed structural integration would also be insufficient. If underlying biological processes are of interest, cells such as macrophages (M1, M2), FBGCs and neutrophil granulocytes should be evaluated and more detailed examination techniques additionally used. On the other hand, we evaluated chronic degenerative changes in tendons with the focus on underlying pathological processes of the disease. In these studies *e.g.* FBGCs are negligible. Changes in collagen structure or composition are important as well as vascularisation and infiltration of inflammatory cells. They will give an indication of progression of the disease.

AI-based methods might help to yield more objective results for collagen structure or cell counting, if slices and stainings are homogeneous. They might enhance comparability and objective quantitative evaluation. However, histological samples from clinical patients or even *in vivo* studies are often inhomogeneous *e.g.* in their structure and cutting direction. Depending on the exact location, structure will differ without underlying different pathological conditions. In case of immunostaining, background fluorescence and intensity of specific signal might influence exposure times in different slices. These are only some examples which might complicate a completely standardised AI-based procedure. However, in our opinion there is a need to enhance comparability between studies by establishing uniform evaluation guidelines and collagen structure, vascularity and cellular infiltration are the most important issues in most research questions and yield the most robust results in semi-quantitative scoring.

Gundula Schulze-Tanzil: Do fatty inclusions play a role in degenerated enthesis?

Authors: Fatty inclusions (or infiltrations) do not play a role in the degenerated enthesis itself. There is a great heterogeneity in reporting histopathological changes in tendinopathy. However, there are some semi-quantitative scores available that are used in the literature (*e.g.* Zabrzyńska *et al.*, 2021, additional

reference). Fatty infiltration is not part of the evaluation of the enthesis. However fatty infiltrations are important for another part of the muscle-bone junction: the muscle itself. After tendon rupture, especially full-tear ruptures, the muscles are inactive and chronic changes occur progressively, with fatty infiltration of the muscle tissue being one of the most common changes. The degree of fatty degeneration of the muscle tissue is one of the common parameters when evaluating the chronicity of changes (Barry *et al.*, 2013; Thangarajah *et al.*, 2017; Zumstein *et al.*, 2016, additional references).

Gundula Schulze-Tanzil: How would the authors think about von Kossa and alizarin red stain to show ossifications?
Authors: Both, von Kossa and alizarin red, are common stains to show ossification and are widely used in the literature – and also by the authors' group – to show calcified areas. Although the tendon itself does not contain osseous tissue, pathologies could lead to mineralised/calcified areas within the tendon. While alizarin red is more common in cell culture tests (Durgam *et al.*, 2019; Rui *et al.*, 2013, additional references), it can also be used for the staining of histological tissue samples (Lu *et al.*, 2020, additional reference; Rigueur and Lyons, 2014). In contrast, von Kossa stain is a very common staining technique to visualise ossifications/calcifications within the tissue of the musculoskeletal system (Carvalho *et al.*, 2020; Limraksasin *et al.*, 2020; Schneider, 2021; Yu *et al.*, 2019).

Gundula Schulze-Tanzil: Which role do elastic fibres and their visualisation play in the enthesis?
Authors: Elastic fibres and their visualisation only play a minor role in the enthesis. Elastic fibres are needed at every location where tissue has to adapt to stresses. For example, arteries, after the pulse wave has stretched the vessel walls, have to contract again to maintain a constant total volume. In the enthesis, a tight contact between tendon and bone is needed to allow for an optimal transfer of stresses to enable joint movement with minimal possible force needed. However, elastic fibre content can change during pathological processes and visualisation might give interesting/important information. For example, Svärd *et al.* (2020, additional reference) showed that "Elastin levels are higher in healing tendons than in intact tendons and influence tissue compliance".

Additional References

Barry JJ, BSE, Lansdown DA, MD, Cheung S, MD, Feeley BT, MD, Ma CB, MD (2013) The relationship between tear severity, fatty infiltration, and muscle atrophy in the supraspinatus. J Shoulder Elbow Surg **22**: 18-25.

Durgam SS, Altmann NN, Coughlin HE, Rollins A, Hostnik LD (2019) Insulin enhances the *in vitro* osteogenic capacity of flexor tendon-derived progenitor cells. Stem Cells Int **2019**: 1602751. DOI: 10.1155/2019/1602751.

Lu P, Dai G, Liu J, Rui Y, Chen M, Zhang C, Li Y (2020) Higher BMP expression in tendon stem/progenitor cells contributes to the increased heterotopic ossification in Achilles tendon with aging. Front Cell Dev Biol **8**: 570605. DOI: 10.3389/fcell.2020.570605.

Rui YF, Lui PPY, Wong YM, Tan Q, Chan KM (2013) BMP-2 stimulated non-tenogenic differentiation and promoted proteoglycan deposition of tendon-derived stem cells (TDSCs) *in vitro*. J Orthop Res **31**: 746-753.

Svärd A, Hammerman M, Eliasson P (2020) Elastin levels are higher in healing tendons than in intact tendons and influence tissue compliance. FASEB J **34**: 13409-13418.

Thangarajah T, Henshaw F, Sanghani-Kerai A, Lambert SM, Pendegrass CJ, Blunn GW (2017) Supraspinatus detachment causes musculotendinous degeneration and a reduction in bone mineral density at the enthesis in a rat model of chronic rotator cuff degeneration. Shoulder Elbow **9**: 178-187.

Zabrzyńska M, Grzanka D, Zielińska W, Jaworski Ł, Pękala P, Gagat M (2021) The Bonar score in the histopathological assessment of tendinopathy and its clinical relevance - a systematic review. Medicina (Kaunas) **57**: 367. DOI: 10.3390/medicina57040367.

Zumstein M-, Lädermann A, Raniga S, Schär M- (2016) The biology of rotator cuff healing. Orthop Traumatol Surg Res **103**: S1-S10.

Editor's note: The Guest Editor responsible for this paper was Britt Wildemann.